Event-Triggered Algorithms for Leader-Follower Consensus of Networked Euler-Lagrange Agents

Qingchen Liu, Mengbin Ye, Jiahu Qin and Changbin Yu*

***Abstract*—This paper proposes three different distributed event-triggered control algorithms to achieve leader-follower consensus for a network of Euler-Lagrange agents. We firstly propose two model-independent algorithms for a subclass of Euler-Lagrange agents without the vector of gravitational potential forces. By model-independent, we mean that each agent can execute its algorithm with no knowledge of the agent self-dynamics. A variable-gain algorithm is employed when the sensing graph is undirected; algorithm parameters are selected in a fully distributed manner with much greater flexibility compared to all previous work concerning event-triggered consensus problems. When the sensing graph is directed, a constant-gain algorithm is employed. The control gains must be centrally designed to exceed several lower bounding inequalities which require limited knowledge of bounds on the matrices describing the agent dynamics, bounds on network topology information and bounds on the initial conditions. When the Euler-Lagrange agents have dynamics which include the vector of gravitational potential forces, an adaptive algorithm is proposed. This requires more information about the agent dynamics but allows for the estimation of uncertain agent parameters.**

For each algorithm, a trigger function is proposed to govern the event update times. The controller is only updated at each event, which ensures that the control input is piecewise constant and thus saves energy resources. We analyse each controller and trigger function to exclude Zeno behaviour.

I. Introduction

The field of multi-agent systems has received extensive attention from the control community in the past two decades. In particular, coordination of a network of interacting agents to achieve a global objective has been seen as a key sub-area within the field. See [1] for a recent survey. Leader-follower consensus is a variation of the commonly studied consensus problem where, with all agents having a commonly defined state variable(s), the network of follower agents converges to the state value of the stationary leader. This is achieved by interaction between neighbouring agents using distributed control algorithms [2], [3].

The Euler-Lagrange equations describe the dynamics of a large class of nonlinear systems (including many mechanical systems such as robotic manipulators, spacecraft and marine vessels) [4], [5]. As a result, there is motivation to study multi-agent coordination problems where each agent has Euler-Lagrange dynamics [6]. Leader-follower consensus for directed networks of Euler-Lagrange agents has been studied in [7] using a model-independent controller, and in [8] using an adaptive controller.

Recently, use of event-triggered controllers in multi-agent coordination problems has been popularised [9]–[11]. While each agent has continuous time dynamics, the controller is updated at discrete time instants based on event-scheduling. Because the controller updates occur at specific events, this has the benefit of reducing actuator updates. However, it is important to properly design and analyse the event-scheduling trigger function to exclude Zeno behaviour [12], [13], which can cause the controller to collapse. Numerous results have been published studying consensus based problems using distributed event-triggered control laws. However, the majority study agents with single and double-integrator dynamics [14]–[17].

There have been relatively few results published studying event-triggered control for networks of Euler-Lagrange agents. Pioneering contributions studied leaderless consensus (but not leader-follower consensus) on an undirected network [18], [19]. The dynamics studied in [18] and [19] are a subclass of Euler-Lagrange dynamics as they do not consider the presence of gravitational forces for each agent. While continuous model-independent algorithms e.g. [7] are easily adapted to be event-triggered, as shown in [18], [19], they cannot guarantee the coordination objective in the presence of gravitational forces (which has an effect similar to a bounded disturbance). Typical control techniques required to deal with this term include feedback linearisation [20], adaptive control [8] and sliding mode control [21]. We note that these techniques have not been well studied in an event-triggered framework. In [22], an adaptive, event-triggered controller is proposed to achieve flocking behaviour for undirected networks of Euler-Lagrange agents. This allows for gravitational forces omitted in [18], [19]. However, the proposed controller in [22] is piecewise continuous, which restricts its implementation in digital platforms. Moreover, it is worth noting that the trigger function used in [22] cannot eliminate Zeno behaviour for each agent.

A. *Contributions of This Paper*

In this paper, we propose three different distributed event-triggered control algorithms to achieve leader-follower consensus for networked Euler-Lagrange agents; each algorithm has different strengths and their appropriateness of use may depend on the application scenario.

*Corresponding author: Changbin Yu.

Q. Liu, M. Ye and C. Yu are with the Research School of Engineering, Australian National University, Canberra ACT 0200, Australia. {qingchen.liu, mengbin.ye, brad.yu}@anu.edu.au. C. Yu is also with the Institute of Advanced Technology, Westlake Institute for Advanced Study, Zhejiang, China.

J. Qin is with the Department of Automation, University of Science and Technology of China, Hefei 230027, China. jhqin@ustc.edu.cn

We propose two model-independent controllers for Euler-Lagrange agents without the gravitational term. Firstly, a globally asymptotically stable variable-gain algorithm is proposed for agents on undirected graphs. The variable-gain controller allows for fully distributed *and arbitrary design of parameters in* both the control algorithm and trigger function. *For agents with complex dynamics, almost all existing results require centralised design of key parameters in the trigger function using limited global knowledge of the network [18], [19], [22]. The design of these key parameters is to ensure either Zeno-free behaviour, or to guarantee convergence of the controller. In the case of simple agent dynamics, the parameters are distributed in design but must either obey upper or lower bounds [14]–[16], [23].* As such, the fully distributed variable-gain controller represents a significant advance on existing event-triggered control algorithms, because stability, convergence and Zeno-free behaviour are always guaranteed, even if the algorithm and trigger function parameters are arbitrarily selected.

Even when implemented continuously, and with simple agent dynamics, variable-gain algorithms on directed graphs are difficult to analyse [24]–[26]. For the second model-independent controller, which is applicable for directed graphs, we are therefore motivated to use constant control gains. It will become apparent in the sequel that, even with constant gains, the combination of Euler-Lagrange dynamics, directed topology, and event-based control requires nontrival stability analysis. The algorithm achieves leader-follower consensus semi-globally, exponentially fast (neither directed graphs nor exponential stability has been studied in any existing results on event-triggered controller of Euler-Lagrange agents). Some limited knowledge of the bounds on the agent dynamic parameters, the network topology and a set of all possible initial conditions is required to centrally design the control gains. This is a trade-off for allowing agents to interact on a directed graph.

Lastly, we propose a globally asymptotically stable adaptive algorithm for use when the gravitational term is present in the agent self-dynamics; this algorithm appeared in our preliminary work [27]. The adaptive algorithm is able to estimate uncertain dynamical parameters, but requires increased knowledge about the agent self-dynamics.

All three proposed controllers are piecewise constant (unlike the piecewise continuous algorithm in [22]), which has the benefit of reducing actuator updates and thus conserving energy resources. Furthermore, each agent only requires state, and relative state measurements, and does not require knowledge of the trigger times of neighbouring agents (unlike [18], [22]), which in general reduces the number of controller updates. For each algorithm, a trigger function is proposed and we show that Zeno behaviour can be excluded for every agent. All three trigger functions are of the same form with only minor modifications. Each term of the trigger function is carefully selected to ensure that the trigger function is more effective, when compared with existing trigger functions which do one of the following, but not both: 1) reduce the total number of events, and 2) eliminate Zeno behaviour for every agent. We show this by detailed comparison and analysis based on simulations. As a result of having multiple terms in the trigger function to achieve the aforementioned improvements, the stability analysis is significantly more complex. Each algorithm requires a different approach to proving stability, and the proposed methods may be useful for other problems in event-based control of multi-agent systems.

Due to a limited number of pages, some proofs and additional simulations are omitted from this paper and are available in an extended version of this paper on arXiv [28].

B. Structure of the Rest of the Paper

Section II provides mathematical notations and background on graph theory and Euler-Lagrange systems. A formal problem definition is also provided. The three different distributed event-triggered control algorithms are then proposed and analysed in Section III, IV and V, separately. Concluding remarks are given in Section VI.

II. Background and problem statement

A. Notations and Mathematical Preliminaries

In this paper, $\mathbb{R}^n$ denotes the n-dimensional Euclidean space and $\mathbb{R}^{m\times n}$ denotes the set of $m \times n$ real matrices. The transpose of a vector or matrix $\boldsymbol{A}$ is given by $\boldsymbol{A}^\top$. The i^{th} smallest eigenvalue of a symmetric matrix $\boldsymbol{A}$ is denoted by $\lambda_i(\boldsymbol{A})$. Let $\boldsymbol{x} = [\boldsymbol{x}_1, \dots, \boldsymbol{x}_n]^\top$ where $\boldsymbol{x}_i \in \mathbb{R}^{n\times n}$ and $n \geq 1$. Then $diag\{\boldsymbol{x}\}$ denotes a (block) diagonal matrix with the (block) elements of $\boldsymbol{x}$ on its diagonal, i.e. $diag\{\boldsymbol{x}_1, ..., \boldsymbol{x}_n\}$. A symmetric matrix $\boldsymbol{A} \in \mathbb{R}^{n\times n}$ which is positive definite (respectively non-negative definite) is denoted by $\boldsymbol{A} > 0$ (respectively $\boldsymbol{A} \geq 0$). For two symmetric matrices $\boldsymbol{A}, \boldsymbol{B}$, the expression $\boldsymbol{A} > \boldsymbol{B}$ is equivalent to $\boldsymbol{A} - \boldsymbol{B} > 0$. The $n \times n$ identity matrix is $\boldsymbol{I}_n$ and $\mathbf{1}_n$ denotes an n-tuple column vector of all ones. The $n \times 1$ column vector of all zeros is denoted by $\mathbf{0}_n$. The symbol $\otimes$ denotes the Kronecker product. The Euclidean norm of a vector, and the matrix norm induced by the Euclidean norm, are denoted by $\|\cdot\|$. The absolute value of a real number is $|\cdot|$. For the space of piecewise continuous, bounded vector functions, the norm is defined as $\|f\|_{\mathcal{L}_\infty} = \sup \|f(t)\| < \infty$ and the space is denoted by $\mathcal{L}_\infty$. The space $\mathcal{L}_p$ for $1 \leq p < \infty$ is defined as the set of all piecewise continuous vector functions such that $\|f\|_{\mathcal{L}_p} = \left(\int_0^\infty \|f(t)\|^p dt\right)^{1/p} < \infty$ where p refers to the type of p-norm.

We provide a theorem and a lemma, which will be used in this paper.

Theorem 1 (Mean Value Theorem for Vector-Valued Functions [29])**.** *For a continuous vector-valued function $\boldsymbol{f}(s) : \mathbb{R} \to \mathbb{R}^n$ differentiable on $s \in [a, b]$, there exists $t \in (a, b)$ such that*

$$\left\| \frac{d\boldsymbol{f}}{ds}(t) \right\| \geq \frac{1}{b-a} \|\boldsymbol{f}(b) - \boldsymbol{f}(a)\|$$

Lemma 1 (From [30])**.** *If a function $f(t)$ satisfies $f(t), \dot{f}(t) \in \mathcal{L}_\infty$, and $f(t) \in \mathcal{L}_p$ for some value of $p \in [1, \infty)$, then $f(t) \to 0$ as $t \to \infty$.*

B. Graph Theory

We model the interactions among the leader and n followers by a weighted directed graph (digraph) $\mathcal{G} = (\mathcal{V}, \mathcal{E}, \mathcal{A})$ with vertex set $\mathcal{V} = \{v_0, v_1, \cdots, v_n\}$ and edge set $\mathcal{E} \subseteq \mathcal{V} \times \mathcal{V}$. Without loss of generality, the leader agent is numbered by v_0. We use $\mathcal{G}_F$ to describe the interactions among the n follower agents with vertex set $\mathcal{V}_F = \{v_1, \cdots, v_n\}$ and edge set $\mathcal{E}_F \subseteq \mathcal{V}_F \times \mathcal{V}_F$. An ordered edge set of $\mathcal{G}$ is $e_{ij} = (v_i, v_j)$. The weighted adjacency matrix $\mathcal{A} = \mathcal{A}(\mathcal{G}) = \{a_{ij}\}$ is the $(n+1) \times (n+1)$ matrix given by $a_{ij} > 0$, if $e_{ji} \in \mathcal{E}$ and $a_{ij} = 0$, otherwise. In this paper, it is assumed that $a_{ii} = 0$, i.e. there are no self-loops. The edge e_{ij} is incoming with respect to v_j and outgoing with respect to v_i. A graph is undirected if $e_{ij} \in \mathcal{E} \Leftrightarrow e_{ji} \in \mathcal{E}$ and $a_{ij} = a_{ji}$. The neighbour set of v_i is denoted by $\mathcal{N}_i = \{v_j \in \mathcal{V} : (v_i, v_j) \in \mathcal{E}\}$. The $(n+1)\times(n+1)$ Laplacian matrix, $\mathcal{L} = \{l_{ij}\}$, of the associated directed graph $\mathcal{G}$ is defined as $l_{ij} = -a_{ij}$ for all $i \neq j$ and $l_{ii} = \sum_{k=1,k\neq i}^{n} a_{ik}$ for all i. A digraph with $n+1$ vertices is called a directed spanning tree if it has n edges and there exists a root vertex with directed paths to every other vertex [6]. The following result holds for the Laplacian matrix associated with a directed graph.

Lemma 2 (From [6])**.** *Let $\mathcal{L}$ be the Laplacian matrix associated with a directed graph $\mathcal{G}$. Then $\mathcal{L}$ has a simple zero eigenvalue and all other eigenvalues have positive real parts if and only if $\mathcal{G}$ has a directed spanning tree.*

Lemma 3 (From [31])**.** *Suppose a graph $\mathcal{G}$ contains a directed spanning tree, and there are no edges of $\mathcal{G}$ which are incoming to the root vertex v_0 of the tree. Then the Laplacian matrix associated with $\mathcal{G}$ has the following form:*

$$\mathcal{L} = \begin{bmatrix} 0 & \mathbf{0}_n^T \\ \mathcal{L}_{21} & \mathcal{L}_{22} \end{bmatrix}$$

and all eigenvalues of $\mathcal{L}_{22}$ have positive real parts. Moreover, there exists a diagonal positive definite matrix $\boldsymbol{\Gamma}$ such that $\boldsymbol{Q} := \boldsymbol{\Gamma}\mathcal{L}_{22} + \mathcal{L}_{22}^\top \boldsymbol{\Gamma} > 0$. In addition, if $\mathcal{G}_F$ is undirected, then $\mathcal{L}_{22}$ is symmetric positive definite.

C. Euler-Lagrange Systems

A class of dynamical systems can be described using the Euler-Lagrange equations [4]. The general form for the i^{th} agent equation of motion is:

$$\boldsymbol{M}_i(\boldsymbol{q}_i)\ddot{\boldsymbol{q}}_i + \boldsymbol{C}_i(\boldsymbol{q}_i, \dot{\boldsymbol{q}}_i)\dot{\boldsymbol{q}}_i + \boldsymbol{g}_i(\boldsymbol{q}_i) = \boldsymbol{\tau}_i \tag{1}$$

where $\boldsymbol{q}_i \in \mathbb{R}^p$ is a vector of the generalized coordinates, $\boldsymbol{M}_i(\boldsymbol{q}_i) \in \mathbb{R}^{p\times p}$ is the inertial matrix, $\boldsymbol{C}_i(\boldsymbol{q}_i, \dot{\boldsymbol{q}}_i) \in \mathbb{R}^{p\times p}$ is the Coriolis and centrifugal torque matrix, $\boldsymbol{g}_i(\boldsymbol{q}_i) \in \mathbb{R}^p$ is the vector of gravitational forces and $\boldsymbol{\tau}_i \in \mathbb{R}^p$ is the control input vector. For agent i, we have $\boldsymbol{q}_i = [\boldsymbol{q}_i^{(1)}, \ldots, \boldsymbol{q}_i^{(p)}]^\top$. We assume each agent is fully actuated. Throughout this paper, the dynamics in (1) are assumed to satisfy the following properties, details of which are provided in [4].

- P1 The matrix $\boldsymbol{M}_i(\boldsymbol{q}_i)$ is symmetric positive definite.
- P2 There exist constants $k_{\underline{m}}, k_{\overline{M}} > 0$ such that $k_{\underline{m}}\boldsymbol{I}_p \leq \boldsymbol{M}_i(\boldsymbol{q}_i) \leq k_{\overline{M}}\boldsymbol{I}_p, \forall i, \boldsymbol{q}_i$. It follows that $\sup_{\boldsymbol{q}_i} \|\boldsymbol{M}_i\|_2 \leq k_{\overline{M}}$ and $k_{\underline{m}} \leq \inf_{\boldsymbol{q}_i} \|\boldsymbol{M}_i^{-1}\|_2{}^{-1}\ \forall i$.
- P3 There exists a constant $k_C > 0$ such that $\|\boldsymbol{C}_i\|_2 \leq k_C \|\dot{\boldsymbol{q}}_i\|_2, \forall i, \dot{\boldsymbol{q}}_i$.
- P4 The matrix $\boldsymbol{C}_i(\boldsymbol{q}_i, \dot{\boldsymbol{q}}_i)$ is related to the inertial matrix $\boldsymbol{M}_i(\boldsymbol{q}_i, \dot{\boldsymbol{q}}_i)$ by the expression $\boldsymbol{x}^T(\frac{1}{2}\dot{\boldsymbol{M}}_i(\boldsymbol{q}_i) - \boldsymbol{C}_i(\boldsymbol{q}_i, \dot{\boldsymbol{q}}_i))\boldsymbol{x} = 0$ for any $\boldsymbol{q}, \dot{\boldsymbol{q}}, \boldsymbol{x} \in \mathbb{R}^p$. This implies that $\dot{\boldsymbol{M}}_i(\boldsymbol{q}_i) = \boldsymbol{C}_i(\boldsymbol{q}_i, \dot{\boldsymbol{q}}_i) + \boldsymbol{C}_i(\boldsymbol{q}_i, \dot{\boldsymbol{q}}_i)^\top$.
- P5 There exists a constant $k_g > 0$ such that $\|\boldsymbol{g}_i(\boldsymbol{q}_i)\| < k_g$.
- P6 Linearity in the parameters: $\boldsymbol{M}_i(\boldsymbol{q}_i)\boldsymbol{x} + \boldsymbol{C}_i(\boldsymbol{q}_i, \dot{\boldsymbol{q}}_i)\boldsymbol{y} + \boldsymbol{g}_i(\boldsymbol{q}_i) = \boldsymbol{Y}_i(\boldsymbol{q}_i, \dot{\boldsymbol{q}}_i, \boldsymbol{x}, \boldsymbol{y})\boldsymbol{\Theta}_i$ for all vectors $x, y \in \mathbb{R}^p$, where $\boldsymbol{Y}_i(\boldsymbol{q}_i, \dot{\boldsymbol{q}}_i, \boldsymbol{x}, \boldsymbol{y})$ is the known regressor matrix and $\boldsymbol{\Theta}_i$ is a vector of unknown but constant parameters associated with the i^{th} agent.

Assumption 1. *(Sub-class of dynamics) In Sections III and IV, we assume that $\boldsymbol{g}_i(\boldsymbol{q}_i) = \boldsymbol{0}, \forall i$. In other words, the dynamics of the agents belong to a subclass of Euler-Lagrange equations which do not have a gravity term. That is,*

$$\boldsymbol{M}_i(\boldsymbol{q}_i)\ddot{\boldsymbol{q}}_i + \boldsymbol{C}_i(\boldsymbol{q}_i, \dot{\boldsymbol{q}}_i)\dot{\boldsymbol{q}}_i = \boldsymbol{\tau}_i \tag{2}$$

If the gravity term $\boldsymbol{g}_i(\boldsymbol{q}_i)$ is present, the adaptive controller proposed in Section V may be used.

D. Problem Statement

Denote the leader as agent 0 with $\boldsymbol{q}_0$ and $\dot{\boldsymbol{q}}_0$ being the generalised coordinates and generalised velocity of the leader, respectively. The aim is to develop event-triggered, distributed algorithms for each Euler-Lagrange follower agent, where the updates are such that τ_i is piecewise-constant. The distributed algorithms are designed to achieve leader-follower consensus to a stationary leader, i.e. $\dot{\boldsymbol{q}}_0(t) = 0, \forall t \geq 0$. Leader-follower consensus is said to be achieved if $\lim_{t\to\infty} \|\boldsymbol{q}_i(t) - \boldsymbol{q}_0(t)\| = 0, \forall i = 1, \ldots, n$ and $\lim_{t\to\infty} \|\dot{\boldsymbol{q}}_i(t)\| = 0, \forall i = 1, \ldots, n$ are satisfied.

Another aim of this paper is to exclude the possibility of Zeno behaviour, which we will formally below. Roughly speaking, Zeno behaviour of an event-based controller means an infinite number of controller updates occur in a finite time period, which is undesirable since no practical controller can do this.

In this paper, we assume that agent $i \in 1, \ldots, n$ is equipped with sensors which continuously measure the relative generalised coordinates to agent i's neighbours. In other words, $\boldsymbol{q}_i(t) - \boldsymbol{q}_j(t), \forall j \in \mathcal{N}_i$ is available to agent i. In Section IV we also assume that the relative generalised velocities are available, i.e. $\dot{\boldsymbol{q}}_i(t) - \dot{\boldsymbol{q}}_j(t), \forall j \in \mathcal{N}_i$. The scenario where agents collect relative information to execute algorithms can be found in many experimental testbeds, such as ground robots or UAVs equipped with high-speed cameras. It is also assumed that each agent i can measure its own generalised velocity continuously, i.e. $\dot{\boldsymbol{q}}_i(t)$.

III. Variable-gain, model-independent controller on undirected networks

In this section, we introduce a variable-gain, event-triggered control algorithm for when the network model of the follower agents is described by an undirected graph. We show that the proposed algorithm does not require any knowledge of the multi-agent system (i.e totally distributed design) and is globally stable. Zeno behaviour is also excluded for each agent in the system.

A. Main Result

Define a new state variable for agent i as

$$\boldsymbol{z}_i(t) = \sum_{j=0}^{n} a_{ij}(\boldsymbol{q}_i(t) - \boldsymbol{q}_j(t)) + \mu_i(t)\dot{\boldsymbol{q}}_i(t), \qquad i = 1, \ldots, n$$

where a_{ij} is the (i,j)th element of the adjacency matrix $\mathcal{A}$ associated with the digraph $\mathcal{G}$. Note that the follower graph $\mathcal{G}_F$ is undirected. The variable control gain $\mu_i(t)$ is subject to the following updating law[1]:

$$\dot{\mu}_i(t) = \alpha_i \dot{\boldsymbol{q}}_i(t)^\top \dot{\boldsymbol{q}}_i(t) \tag{3}$$

The scalar α_i is strictly positive and may be independent for all agents. It is obvious that $\mu_i(t)$ is a monotonically increasing function. The variable-gain scalar function $\mu_i(t)$ is initialised at $t = 0$ with an arbitrary $\mu_i(0) \geq 0$, which implies that $\mu_i(t) \geq 0, \forall\, t > 0$.

The control algorithm is now proposed. Let the trigger time sequence of agent i be denoted as $t_0^i, t_1^i, \ldots, t_k^i, \ldots$ with $t_0^i := 0$ and we detail below how each trigger time is determined. The event-triggered controller for follower agent i is designed as:

$$\boldsymbol{\tau}_i(t) = -\boldsymbol{z}_i(t_k^i) \tag{4}$$

for $t \in [t_k^i, t_{k+1}^i)$. The control input for each agent is held constant and equal to the last control update $\boldsymbol{\tau}_i(t_k^i)$ in the time interval $[t_k^i, t_{k+1}^i)$.

We define a state mismatch for agent i between consecutive event times t_k^i and t_{k+1}^i as follows:

$$\boldsymbol{e}_i(t) = \boldsymbol{z}_i(t_k^i) - \boldsymbol{z}_i(t) \tag{5}$$

for $t \in [t_k^i, t_{k+1}^i)$. The trigger function is designed as follows:

$$f_i(\boldsymbol{e}_i, \dot{\boldsymbol{q}}_i, \omega_i) = \|\boldsymbol{e}_i(t)\|^2 - \beta_i \|\dot{\boldsymbol{q}}_i(t)\|^2 - \omega_i(t) \tag{6}$$

where β_i is *an arbitrarily chosen positive constant* (see the Proof of **Theorem** 2 for the explanations), $\omega_i(t)$ is an offset function defined as $\omega_i(t) = \kappa_i \exp(-\varepsilon_i t)$ with arbitrarily chosen $\kappa_i, \varepsilon_i > 0$. The k^{th} event for agent i is triggered as soon as the trigger condition $f_i(\boldsymbol{e}_i, \dot{\boldsymbol{q}}_i, \omega_i) = 0$ is satisfied. The control input $\boldsymbol{\tau}_i(t)$ is updated only when an event of agent i is triggered. Furthermore, every time an event is triggered, and in accordance with their definitions, the measurement error $\boldsymbol{e}_i(t)$ is reset to be equal to zero and thus the trigger function assumes a non-positive value, that is, $f_i(\boldsymbol{e}_i, \dot{\boldsymbol{q}}_i, \omega_i) \leq 0$.

[1] In some existing works on multi-agent systems, similar controllers which have monotonically increasing gains have been termed "adaptive-gain controllers" or "adaptive controllers", see e.g. [24], [25], [32]. While we acknowledge this terminology is correct, we choose to call the controller proposed in this section a "variable-gain controller" to differentiate, and avoid confusion with, the controller we will propose in Section V, which adaptively estimates unknown, but constant, parameters of the agent dynamics. The variable-gain controller in this section and the adaptive controller in Section V are fundamentally different in design and ideology.

Definition 1. *Let a finite time interval be $t_{\mathcal{Z}} = [a, b]$ where $0 \leq a < b < \infty$. If, for some finite $k \geq 0$, the sequence of event triggers $\{t_k^i, ..., t_\infty^i\} \in [a, b]$ then the system exhibits Zeno behaviour.*

Remark 1. *In existing event-based multi-agent control literature, the parameters of the state-dependent term are typically restricted. For example, the authors of [19] studied leaderless consensus for undirected networked Euler-Lagrange agents. Different from our proposed variable-gain controller, their controller adopts fixed gains. As a result, the parameter ϱ_i (see the trigger function in [19]) of the state-dependent term has to be less than a computable upper bound. This bound requires knowledge of the control gains and graph topology (e.g. number of neighbours and degree of the agent). In comparison, our equivalent parameter β_i in our proposed trigger function* (6) *can be chosen as an arbitrarily positive constant. This provides a much greater flexibility in the implementation of the algorithm.*

We note that even in papers considering simple single integrator dynamics with a parameter for the state-dependent term, equivalent to our β_i, require an upper bound as well (see the seminal works of [14], [16]). To the best of the authors' knowledge, the event-based controller proposed in this paper is the first to allow for an arbitrarily chosen positive parameter for the state-dependent term in the trigger function.

By substituting the control input (4) into the system dynamics (2), the closed-loop system can be written as

$$\boldsymbol{M}_i(\boldsymbol{q}_i)\ddot{\boldsymbol{q}}_i(t) + \boldsymbol{C}_i(\boldsymbol{q}_i, \dot{\boldsymbol{q}}_i)\dot{\boldsymbol{q}}_i(t) = -\boldsymbol{z}_i(t_k^i) \tag{7}$$

Then by applying (5), we obtain

$$\boldsymbol{M}_i(\boldsymbol{q}_i)\ddot{\boldsymbol{q}}_i(t) + \boldsymbol{C}_i(\boldsymbol{q}_i, \dot{\boldsymbol{q}}_i)\dot{\boldsymbol{q}}_i(t) = -(\boldsymbol{z}_i(t) + \boldsymbol{e}_i(t)) \tag{8}$$

Define new state variables $\boldsymbol{u}_i = \boldsymbol{q}_i - \boldsymbol{q}_0$ and $\boldsymbol{v}_i = \dot{\boldsymbol{q}}_i$ and we henceforth drop the argument t for brevity, and where there is no confusion. Define the stacked column vectors of all $\boldsymbol{u}_i, \boldsymbol{v}_i, \boldsymbol{q}_i, \boldsymbol{e}_i$ as $\boldsymbol{u} = [\boldsymbol{u}_1^\top, ..., \boldsymbol{u}_n^\top]^\top$, $\boldsymbol{v} = [\boldsymbol{v}_1^\top, ..., \boldsymbol{v}_n^\top]^\top$, $\boldsymbol{q} = [\boldsymbol{q}_1^\top, ..., \boldsymbol{q}_n^\top]^\top$, $\boldsymbol{z} = [\boldsymbol{z}_1^\top, ..., \boldsymbol{z}_n^\top]^\top$ and $\boldsymbol{e} = [\boldsymbol{e}_1^\top, ..., \boldsymbol{e}_n^\top]^\top$ respectively. It is easy to obtain that

$$\begin{aligned}\boldsymbol{z} &= (\mathcal{L}_{22} \otimes \boldsymbol{I}_p)(\boldsymbol{q} - \boldsymbol{1}_n \otimes \boldsymbol{q}_0) + \boldsymbol{K}\dot{\boldsymbol{q}} \\ &= (\mathcal{L}_{22} \otimes \boldsymbol{I}_p)\boldsymbol{u} + \boldsymbol{K}\boldsymbol{v}\end{aligned}$$

where $\boldsymbol{K} = \text{diag}[\mu_1 \boldsymbol{I}_p, ..., \mu_n \boldsymbol{I}_p]$. Define the following block diagonal matrices $\boldsymbol{M}(\boldsymbol{q}) = \text{diag}[\boldsymbol{M}_1(\boldsymbol{q}_1), ..., \boldsymbol{M}_n(\boldsymbol{q}_n)]$, $\boldsymbol{C}(\boldsymbol{q}, \dot{\boldsymbol{q}}) = \text{diag}[\boldsymbol{C}_1(\boldsymbol{q}_1, \dot{\boldsymbol{q}}_1), ..., \boldsymbol{C}_n(\boldsymbol{q}_n, \dot{\boldsymbol{q}}_n)]$. It is obvious that $\boldsymbol{M}$ is symmetric positive definite since $\boldsymbol{M}_i > 0, \forall i$. With these notations, the compact form of system (8) can be expressed as

$$\begin{aligned}\dot{\boldsymbol{u}} &= \boldsymbol{v} \\ \dot{\boldsymbol{v}} &= -\boldsymbol{M}(\boldsymbol{q})^{-1}\left[\boldsymbol{C}(\boldsymbol{q}, \boldsymbol{v})\boldsymbol{v} + (\mathcal{L}_{22} \otimes \boldsymbol{I}_p)\boldsymbol{u} + \boldsymbol{K}\boldsymbol{v} + \boldsymbol{e}\right] \\ \dot{\boldsymbol{K}} &= \boldsymbol{\Xi} \otimes \boldsymbol{I}_p\end{aligned} \tag{9}$$

where $\boldsymbol{\Xi} = \text{diag}[\alpha_1 \|\boldsymbol{v}_1\|_2{}^2, \alpha_2 \|\boldsymbol{v}_2\|_2{}^2, ..., \alpha_n \|\boldsymbol{v}_n\|_2{}^2]$. The leader-follower objective is achieved when there holds $\boldsymbol{u} \equiv \boldsymbol{v} \equiv \boldsymbol{0}_{np}$. We now present the main result for this Section.

Theorem 2. *Suppose that each follower agent with dynamics* (2)*, under Assumption 1, employs the controller* (4) *with trigger function* (6)*. Suppose further that the directed graph $\mathcal{G}$ contains a directed spanning tree, with the leader agent* 0 *as the root node (thus with no incoming edges) and the follower graph $\mathcal{G}_F$ is undirected. Then the leader-follower consensus objective is globally asymptotically achieved and no agent will exhibit Zeno behaviour.*

Proof. We divide our proof into two parts. In the first part, we focus on the stability analysis of the system (9). In the second part, analysis is provided to show the exclusion of Zeno behaviour *for each agent*.

1) Stability analysis: Consider the following Lyapunov-like function

$$\begin{aligned} V &= \frac{1}{2}\boldsymbol{u}^\top(\mathcal{L}_{22}\otimes \boldsymbol{I}_p)\boldsymbol{u} + \frac{1}{2}\boldsymbol{v}^\top \boldsymbol{M}\boldsymbol{v} + \sum_{i=1}^{n}\frac{1}{2\alpha_i}(\mu_i - \bar{\mu})^2 \\ &= V_1 + V_2 + V_3 \end{aligned} \tag{10}$$

where $\bar{\mu}$ is a strictly positive constant. The choice of $\bar{\mu}$ will be presented below. Since $\mathcal{G}$ contains a directed spanning tree and $\mathcal{G}_F$ is undirected, according to **Lemma** 3, $\mathcal{L}_{22}$ is positive definite. Note that $\boldsymbol{M}$ is positive definite and V_3 is non-negative, we conclude that V is strictly positive for nonzero $\boldsymbol{u}$ and $\boldsymbol{v}$.

Taking the derivative of V with respect to time, along the trajectory of system (9), there holds $\dot{V} = \dot{V}_1 + \dot{V}_2 + \dot{V}_3$. Evaluating $\dot{V}_1$ yields $\dot{V}_1 = \boldsymbol{u}^\top(\mathcal{L}_{22}\otimes \boldsymbol{I}_p)\boldsymbol{v}$. Next, the derivative $\dot{V}_2$ is evaluated to be $\dot{V}_2 = \boldsymbol{v}^\top\boldsymbol{M}\dot{\boldsymbol{v}} + \frac{1}{2}\boldsymbol{v}^\top\dot{\boldsymbol{M}}\boldsymbol{v}$, which on further analysis, yields

$$\begin{aligned} \dot{V}_2 &= -\boldsymbol{v}^\top\boldsymbol{C}\boldsymbol{v} - \boldsymbol{v}^\top(\mathcal{L}_{22}\otimes \boldsymbol{I}_p)\boldsymbol{u} - \boldsymbol{v}^\top\boldsymbol{K}\boldsymbol{v} - \boldsymbol{v}^\top\boldsymbol{e} + \frac{1}{2}\boldsymbol{v}^\top\dot{\boldsymbol{M}}\boldsymbol{v} \\ &= -\boldsymbol{v}^\top(\mathcal{L}_{22}\otimes \boldsymbol{I}_p)\boldsymbol{u} - \boldsymbol{v}^\top\boldsymbol{K}\boldsymbol{v} - \boldsymbol{v}^\top\boldsymbol{e} \end{aligned}$$

Lastly, we obtain $\dot{V}_3 = \sum_{i=1}^{n}(\mu_i - \bar{\mu})\boldsymbol{v}_i^\top\boldsymbol{v}_i = \boldsymbol{v}^\top\boldsymbol{K}\boldsymbol{v} - \bar{\mu}\boldsymbol{v}^\top\boldsymbol{v}$. Since $\mathcal{L}_{22}$ is symmetric, summing $\dot{V}_1$, $\dot{V}_2$ and $\dot{V}_3$ yields $\dot{V} = -\bar{\mu}\boldsymbol{v}^\top\boldsymbol{v} + \boldsymbol{v}^\top\boldsymbol{e}$. By using the inequality $\boldsymbol{v}^\top\boldsymbol{e} \le \frac{a}{2}\|\boldsymbol{v}\|^2 + \frac{1}{2a}\|e\|^2, \forall a > 0$, we obtain

$$\dot{V} \le (\frac{a}{2} - \bar{\mu})\|\boldsymbol{v}\|^2 + \frac{1}{2a}\|\boldsymbol{e}\|^2$$

Note that the non-positivity of $f_i(\boldsymbol{e}_i, \boldsymbol{v}_i, \omega_i)$ guarantees that $\|\boldsymbol{e}\|^2 \le \beta\|\boldsymbol{v}\|^2 + \bar{\omega}(t)$, where $\beta = \max_i\{\beta_i\}$ and $\bar{\omega}(t) = \sum_{i=1}^{n}\omega_i(t)$. It follows that $\dot{V}$ satisfies

$$\dot{V} \le (\frac{a}{2} + \frac{\beta}{2a} - \bar{\mu})\|\boldsymbol{v}\|^2 + \bar{\omega}(t)$$

For notation simplicity, we define $\chi = \bar{\mu} - \frac{a}{2} - \frac{\beta}{2a}$. Note that for any given a and β, we can find a sufficiently large $\bar{\mu}$ to ensure $\chi > 0$ and thus

$$\dot{V} \le -\chi\|\boldsymbol{v}\|^2 + \bar{\omega}(t)$$

and it is straightforward to conclude that the parameter β_i in the trigger function (6) can be selected as an arbitrarily positive constant. Integrating both sides of the above equation from zero to t, for any $t > 0$, yields

$$V(t) + \chi\int_0^t \|\boldsymbol{v}(\epsilon)\|^2.\mathrm{d}\epsilon \le V(0) + \sum_{i=1}^{n}\frac{\kappa_i}{\varepsilon_i}$$

which implies that $V(t)$ and $\chi\int_0^t \|\boldsymbol{v}(\epsilon)\|^2.\mathrm{d}\epsilon$ are bounded since $V(0), \kappa_i, \varepsilon_i$ are all bounded. By recalling (10), it is straightforward to conclude that $\boldsymbol{u}, \boldsymbol{v}, \mu_i$ are all bounded. Now we turn to $\dot{\boldsymbol{v}}_i$. Notice that $\dot{\boldsymbol{q}}_0 = 0$ and from (7), we have

$$\dot{\boldsymbol{v}}_i = -\boldsymbol{M}_i(\boldsymbol{q}_i)^{-1}[\boldsymbol{C}_i(\boldsymbol{q}_i, \dot{\boldsymbol{q}}_i)\dot{\boldsymbol{q}}_i + \boldsymbol{z}_i(t_k^i)] \tag{11}$$

Since $\boldsymbol{u}, \boldsymbol{v}, \mu_i$ are bounded, $\dot{\boldsymbol{q}}_i$ and $\boldsymbol{z}_i(t_k^i)$ are bounded. Then by recalling properties P2 and P3, we conclude that $\dot{\boldsymbol{v}}$ is bounded. From the fact that both $\boldsymbol{v}$ and $\dot{\boldsymbol{v}}$ are bounded, we obtain $\boldsymbol{v}, \dot{\boldsymbol{v}} \in \mathcal{L}_\infty$. Moreover, the boundedness of $\chi\int_0^t \|\boldsymbol{v}(\epsilon)\|^2.\mathrm{d}\epsilon$ indicates $\boldsymbol{v} \in \mathcal{L}_2$. By applying **Lemma** 1, we conclude that $\boldsymbol{v} \to \boldsymbol{0}_{np}$ as $t \to \infty$. From (3) we observe that μ_i is strictly monotonically increasing. Combining this with the fact that $\mu_i(0) \ge 0$ is bounded, we conclude that $\mu_i(t), \forall\, i$ tends to a finite constant value as $t \to \infty$.

Now we turn to prove that $\boldsymbol{u} \to \boldsymbol{0}_{np}$. Due to the difficulty arising from the term $\omega_i(t)$ (which makes the system non-autonomous), and the second-order non-linear dynamics, the proof is more complex than existing proofs for showing convergence to the consensus objective. We discuss the intuition behind the following steps in Remark 2 below. Consider firstly $\boldsymbol{e}$ and $\boldsymbol{K}$. By recalling the definitions of $\boldsymbol{e}_i$ and the trigger function f_i, we observe that $\|\boldsymbol{e}\|^2 \le \beta\|\boldsymbol{v}\|^2 + \bar{\omega}(t), \forall\, t$. We concluded above that $\lim_{t\to\infty}\|\boldsymbol{v}\|, \bar{\omega}(t) = 0$ which implies that $\lim_{t\to\infty}\boldsymbol{e} = \boldsymbol{0}_{np}$. Recalling the definition of $\boldsymbol{K}$ above (9), and the fact that $\mu_i, \forall\, i$ tends to a constant value as $t \to \infty$, we conclude that $\lim_{t\to\infty}\boldsymbol{K} = \bar{\boldsymbol{K}}$ where $\bar{\boldsymbol{K}}$ is some finite constant matrix. Rewrite the second equation of (9) as

$$\dot{\boldsymbol{v}} = \boldsymbol{f}(t) + \boldsymbol{r}(t) \tag{12}$$

where $\boldsymbol{f}(t) = -\boldsymbol{M}(\boldsymbol{q})^{-1}(\mathcal{L}_{22}\otimes \boldsymbol{I}_p)\boldsymbol{u}$ and $\boldsymbol{r}(t) = -\boldsymbol{M}(\boldsymbol{q})^{-1}\big[\boldsymbol{C}(\boldsymbol{q}, \boldsymbol{v})\boldsymbol{v} + \boldsymbol{K}\boldsymbol{v} + \boldsymbol{e}\big]$ are both vector functions. Since $\lim_{t\to\infty}\boldsymbol{v}, \boldsymbol{e} = \boldsymbol{0}_{np}$, $\bar{\boldsymbol{K}}$ is finite, and $\boldsymbol{M}, \boldsymbol{C}$ are bounded according to Properties P2 and P3, it is obvious that $\lim_{t\to\infty}\boldsymbol{r}(t) = \boldsymbol{0}_{np}$. Then by integrating both sides of (12) from t to $t + \Delta$, where Δ is a finite positive constant and $t \ge 0$, we obtain

$$\boldsymbol{v}(t+\Delta) - \boldsymbol{v}(t) = \int_t^{t+\Delta}\boldsymbol{f}(s)\mathrm{d}s + \int_t^{t+\Delta}\boldsymbol{r}(s).\mathrm{d}s \tag{13}$$

This implies that there holds

$$\left\|\int_t^{t+\Delta}\boldsymbol{f}(s)\mathrm{d}s\right\| \le \|\boldsymbol{v}(t+\Delta) - \boldsymbol{v}(t)\| + \left\|\int_t^{t+\Delta}\boldsymbol{r}(s)\mathrm{d}s\right\| \tag{14}$$

Consider the term $\|\int_t^{t+\Delta}\boldsymbol{f}(s)\mathrm{d}s\|$. By applying **Theorem** 1, we conclude that there holds

$$\left\|\int_t^{t+\Delta}\boldsymbol{f}(s)\mathrm{d}s\right\| \le \Delta\|\boldsymbol{f}(t+\theta(t))\|$$

where $\theta(t) \in (0, \Delta)$. Subtracting $\Delta\|\boldsymbol{f}(t)\|$ from the both sides of the above inequality yields

$$\left\|\int_t^{t+\Delta}\boldsymbol{f}(s)\mathrm{d}s\right\| - \Delta\|\boldsymbol{f}(t)\| \le \Delta\left(\|\boldsymbol{f}(t+\theta(t))\| - \|\boldsymbol{f}(t)\|\right)$$

Considering the above right hand side, we observe that $\Delta\left(\|\boldsymbol{f}(t+\theta(t))\|-\|\boldsymbol{f}(t)\|\right) \leq \Delta\|\boldsymbol{f}(t+\theta(t))-\boldsymbol{f}(t)\| = \Delta\|\int_t^{t+\theta(t)}\dot{\boldsymbol{f}}(s)\mathrm{d}s\|$, which implies that

$$\left\|\int_t^{t+\Delta}\boldsymbol{f}(s)\mathrm{d}s\right\| - \Delta\|\boldsymbol{f}(t)\| \leq \Delta\left\|\int_t^{t+\theta(t)}\dot{\boldsymbol{f}}(s)\mathrm{d}s\right\| \quad (15)$$

Note that $\mathrm{d}(\boldsymbol{M}^{-1})/\mathrm{d}t = -\boldsymbol{M}^{-1}\dot{\boldsymbol{M}}\boldsymbol{M}^{-1}$ because $\mathrm{d}(\boldsymbol{M}^{-1}\boldsymbol{M})/\mathrm{d}t = \boldsymbol{M}^{-1}\dot{\boldsymbol{M}} + (\mathrm{d}(\boldsymbol{M}^{-1})/\mathrm{d}t)\boldsymbol{M} = \boldsymbol{0}$. From Properties P3 and P4, we observe that $\lim_{t\to\infty}\|\dot{\boldsymbol{M}}\| \leq 2k_C\|\boldsymbol{v}\| = 0$. Observe that

$$\dot{\boldsymbol{f}} = -\left(\frac{\mathrm{d}(\boldsymbol{M}(\boldsymbol{q})^{-1})}{\mathrm{d}t}(\mathcal{L}_{22}\otimes\boldsymbol{I}_p)\boldsymbol{v} + \boldsymbol{M}(\boldsymbol{q})^{-1}(\mathcal{L}_{22}\otimes\boldsymbol{I}_p)\boldsymbol{v}\right)$$

We proved below (11) that $\boldsymbol{u}$ is bounded and $\lim_{t\to\infty}\boldsymbol{v} = \boldsymbol{0}_{np}$. Recall also that $\|\boldsymbol{M}(\boldsymbol{q})^{-1}\|$ is bounded according to Property P2. It follows that $\lim_{t\to\infty}\|\dot{\boldsymbol{f}}\| = 0$ because $\lim_{t\to\infty}\|\boldsymbol{v}\| = 0$. This implies $\|\int_t^{t+\theta(t)}\dot{\boldsymbol{f}}(s)\mathrm{d}s\| = 0$ since $\theta(t)\in(0,\Delta)$ is finite. The inequality (15) then implies that $\lim_{t\to\infty}\left\|\int_t^{t+\Delta}\boldsymbol{f}(s)\mathrm{d}s\right\| = \Delta\|\boldsymbol{f}(t)\|$. By substituting this into the left hand side of (14), we obtain

$$\Delta\|\boldsymbol{f}(t)\| \leq \|\boldsymbol{v}(t+\Delta)-\boldsymbol{v}(t)\| + \left\|\int_t^{t+\Delta}\boldsymbol{r}(s)\mathrm{d}s\right\| \quad (16)$$

as $t\to\infty$. Immediately above (13), we showed that $\lim_{t\to\infty}\boldsymbol{r} = \boldsymbol{0}_{np}$. In addition, $\lim_{t\to\infty}\boldsymbol{v} = \boldsymbol{0}_{np}$ and Δ is a positive constant. We conclude that $\lim_{t\to\infty}\|\boldsymbol{v}(t+\Delta)-\boldsymbol{v}(t)\| + \left\|\int_t^{t+\Delta}\boldsymbol{r}(s)\mathrm{d}s\right\| = 0$, which according to (16) implies that $\lim_{t\to\infty}\|\boldsymbol{f}(t)\| = 0$. By recalling that $\boldsymbol{f}(t) = -\boldsymbol{M}(\boldsymbol{q})^{-1}(\mathcal{L}_{22}\otimes\boldsymbol{I}_p)\boldsymbol{u}$, we conclude $\lim_{t\to\infty}\boldsymbol{u} = \boldsymbol{0}_{np}$ since both $\boldsymbol{M}(\boldsymbol{q})^{-1}$ and $\mathcal{L}_{22}$ are non-singular. It is obvious that $\lim_{t\to\infty}\boldsymbol{u},\boldsymbol{v} = \boldsymbol{0}_{np}$ implies the leader-follower objective is asymptotically achieved.

2) Absence of Zeno behaviour: According to **Definition** 1, we can prove that Zeno behaviour does not occur for $t\in[0,b]$ by showing that for all $k\geq 0$ there holds $t_{k+1}^i - t_k^i \geq \xi$ where $\xi > 0$ is a strictly positive constant.

Let ξ_i denote the lower bound of the inter-event interval $t_{k+1}^i - t_k^i$ for agent i, i.e. $t_{k+1}^i - t_k^i \geq \xi_i\ ,\forall k : t_k^i \in [0,b]$. In this part of the proof, we show that ξ_i is strictly positive for $k<\infty$ and thus no Zeno behaviour can occur. From the definition of $\boldsymbol{e}_i(t)$ in (5) and the fact that $\boldsymbol{z}_i(t_k^i)$ is a constant, we observe that the derivative of $\|\boldsymbol{e}_i(t)\|$ with respect to time satisfies

$$\frac{d}{dt}\|\boldsymbol{e}_i(t)\| \leq \|\dot{\boldsymbol{z}}_i(t)\| \quad (17)$$

where $\dot{\boldsymbol{z}}_i(t) = \sum_{j=0}^n a_{ij}(\dot{\boldsymbol{q}}_i(t)-\dot{\boldsymbol{q}}_j(t)) + \dot{\mu}_i(t)\dot{\boldsymbol{q}}_i(t) + \mu_i(t)\ddot{\boldsymbol{q}}_i(t),\ i = 1,\ldots,n$. Note that it is straightward to conclude $\dot{\boldsymbol{q}}_i(t),\ddot{\boldsymbol{q}}_i(t),\dot{\mu}_i(t),\mu_i(t)$ are bounded according to the arguments in *Part* 1). This implies $\dot{\boldsymbol{z}}_i(t)$ is bounded. By letting a positive constant B_e represent the upper bound of $\|\dot{\boldsymbol{z}}_i(t)\|$, we obtain

$$\frac{d}{dt}\|\boldsymbol{e}_i(t)\| \leq B_e$$

It follows that

$$\|\boldsymbol{e}_i(t)\| \leq \int_{t_k^i}^t B_e dt = B_e(t-t_k^i) \quad (18)$$

for $t\in[t_k^i, t_{k+1}^i)$ and for any k. It is obvious that the next event time t_{k+1}^i is determined both by the changing rate of $\|\boldsymbol{e}_i(t)\|$ and by the value of the comparison term $\beta_i\|\boldsymbol{v}_i(t)\|^2+\omega_i(t)$ at t_{k+1}^i. Moreover, t_{k+1}^i is the time that

$$\|\boldsymbol{e}_i(t)\|^2 = \beta_i\|\boldsymbol{v}_i(t)\|^2 + \omega_i(t), \qquad t > t_k^i \quad (19)$$

holds. In *Part* 1) we conclude that global state variable $\boldsymbol{v}(t)\to\boldsymbol{0}_{np}$ as $t\to\infty$ but notice that in the evolution of the system (9), the state variable $\boldsymbol{v}_i(t)$ may be equal to $\boldsymbol{0}_p$ instantaneously ($\boldsymbol{v}_i(t)$ is a component of $\boldsymbol{v}(t)$) at t_{k+1}^i. However, this does not imply leader-follower consensus is reached since $\dot{\boldsymbol{v}}_i(t)$ can be non-zero at t_{k+1}^i. We refer to such points in time as "zero-crossing points" for convenience. Here we provide Fig. 2 to show the trigger performance at the zero-crossing points of $\boldsymbol{v}_i(t)$ when $\omega_i(t) = 0$. *It is observed that dense trigger behaviour occurs whenever $\boldsymbol{v}_i(t)$ crosses zero. Theoretically, it can be proved that Zeno behaviour takes place at these zero-crossing points. We refer interested readers to [33] with detailed arguments of the Zeno triggering issues at zero-crossing points.*

Now we return to the trigger time interval analysis. By recalling (19), we conclude that at t_{k+1}^i, the triggering of the event can only occur for the following two cases:

- Case 1: If $\|\boldsymbol{v}_i(t_{k+1}^i)\| \neq 0$, the equality $\|\boldsymbol{e}_i(t_{k+1}^i)\| = \beta_i\|\boldsymbol{v}_i(t_{k+1}^i)\|^2 + \omega_i(t_{k+1}^i)$ is satisfied.
- Case 2: If $\|\boldsymbol{v}_i(t_{k+1}^i)\| = 0$, the equality $\|\boldsymbol{e}_i(t_{k+1}^i)\| = \omega_i(t_{k+1}^i)$ is satisfied.

Compare the above two cases, and note that $\|\boldsymbol{v}_i(t_{k+1}^i)\| > 0$ for any $\|\boldsymbol{v}_i(t_{k+1}^i)\| \neq 0$. By recalling that $\boldsymbol{e}_i(t)$ is equal to zero at t_k^i, it is straightforward to conclude that it takes longer for the quantity $\|e_i(t)\|^2$ to increase to be equal to the quantity $\beta_i\|\boldsymbol{v}_i(t_{k+1}^i)\|^2 + \omega_i(t_{k+1}^i)$ (i.e. Case 1) than to increase to be equal to the quantity $\omega_i(t_{k+1}^i)$ (i.e. Case 2), and thus trigger an event and resetting $\boldsymbol{e}_i(t)$. This implies that $\xi_{Case\,2} < \xi_{Case\,1}$ and proving that there exists a strictly positive $\xi_{Case\,2}$ allows us to draw the conclusion that no Zeno behaviour occurs. According to (18), we have

$$B_e\xi_{Case\,2} \geq \omega_i(t) = \exp(-\kappa_i(t_k^i + \xi_{Case\,2}))$$

This implies that the inter-event time $\xi_{Case\,2}$ is lower bounded by the solution $\xi_{Case\,2}$ of the following equation

$$B_e\xi_{Case\,2} = \exp(-\kappa_i(t_k^i + \xi_{Case\,2})) \quad (20)$$

The solution is time-dependent and strictly positive for any finite time since B_e is strictly positive and upper bounded. Zeno behaviour is thus excluded for all agents. □

Remark 2. *The reader will have noticed the complexity and length of argument required to go from concluding* $\lim_{t\to\infty}\boldsymbol{v} = \boldsymbol{0}_{np}$ *below* (11)*, to concluding* $\lim_{t\to\infty}\boldsymbol{u} = \boldsymbol{0}_{np}$ *below* (16)*. The key reason is the combination of second-order non-linear dynamics and the non-autonomous nature of* (9) *resulting from the offset term* $\omega_i(t)$ *in* (6)*. We now explain the* *intuition for the steps from* (12) *to immediately below* (16)*. Between* (14) *and* (16)*, we use Theorem 1 (mean value inequality for vector-valued functions) and the definition of $\boldsymbol{f}$ to obtain the key equality* $\lim_{t\to\infty}\left\|\int_t^{t+\Delta}\boldsymbol{f}(s)ds\right\| = \Delta\|\boldsymbol{f}(t)\|$*. This allows us to use* (14) *to show a key result:* $\lim_{t\to\infty}\boldsymbol{f} = \mathbf{0}_{np}$ *(because we established earlier the both terms on the right of* (14) *tend to zero). We then use the definition of $\boldsymbol{f}$ to show that* $\boldsymbol{f} = \mathbf{0}_{np} \Rightarrow \boldsymbol{u} = \mathbf{0}_{np}$*.*

The authors in [19] use a similar trigger function with the same offset term, and claim that $\lim_{t\to\infty}\boldsymbol{v} = \mathbf{0}_{np}$ *implies that* $\lim_{t\to\infty}\dot{\boldsymbol{v}} = \mathbf{0}_{np}$*. This is not correct since the system is non-autonomous. The paper [34] uses a trigger function without the offset term, and thus they are able to avoid the non-autonomous issue. However, the lack of the offset term can yield Zeno behaviour, something which was not recorded by [34]. We explore the use of the offset term for avoiding Zeno behaviour in the next section.*

Remark 3. *Unfortunately, we cannot find a constant lower bound for the inter-event time interval. The lower bound ξ_{Case2} found by solving* (20) *is time-dependent and tends to zero as $t\to\infty$. The avoidance of Zeno behaviour depends on the exponential decay offset completely and the trigger performance when $t\to\infty$ is not discussed in the theoretical analysis. However, we note that the state-dependent term in* (6) *provides a performance advantage when $t\to\infty$ due to its own specific effects and should not be removed. We will provide detail explanations for the advantages of our proposed trigger function* (6) *in the following subsection.*

Remark 4. *As with other variable-gain controllers that have monotonically increasing gain, e.g. [24], [25], [32], there is a chance that $\mu_i(t)$ becomes large. This is a fundamental aspect of such controllers, and might be considered a trade-off for being able to design the parameters of the trigger function in a distributed manner. An interesting future work to remedy this problem is to consider an "adaptive σ-modification" algorithm which allows the gain to both increase and decrease, as studied in [25, Section III-C].*

B. Discussions on the choice of trigger functions

In this subsection, we provide discussions regarding the trigger performance of controller (4) using the following three trigger functions

- State-dependent trigger function (SDTF)
$$f_i = \|\boldsymbol{e}_i(t)\| - \beta_i\|\boldsymbol{v}_i(t)\| \tag{21}$$
- Time-dependent trigger function (TDTF)
$$f_i = \|\boldsymbol{e}_i(t)\| - \kappa_i\exp(-\varepsilon_i t) \tag{22}$$
- Mixed trigger function (MTF), which is the proposed (6)
$$f_i = \|\boldsymbol{e}_i(t)\|^2 - \beta_i\|\boldsymbol{v}_i(t)\|^2 - \kappa_i\exp(-\varepsilon_i t) \tag{23}$$

from both the viewpoints of theoretical analysis and numerical simulations. In doing so, we highlight the advantages of our proposed trigger function (6). Note that it is hard, but not impossible, to observe the zero-crossing phenomenon for $\boldsymbol{v}_i(t)\in\mathbb{R}^p, p\geq 2$ (i.e. when $\boldsymbol{v}_i(t) = \mathbf{0}_p$ occurs, Zeno behaviour is observed as discussed in the proof of Theorem 2 and in [33]). This is because each entry of $\boldsymbol{v}_i(t)$ must be simultaneously equal to 0. For purposes of illustration, in this subsection we therefore simulate using dynamics of a one-arm mechanic manipulator ($\boldsymbol{v}_i(t)\in\mathbb{R}^1$). The dynamics are described by equation 3.5 in [4]. For all simulations presented in this subsection, we set a constant step size in MATLAB to be 0.00005 seconds (the numerical accuracy of the simulation) and the running time to be 30 seconds. In order to compare performance, we require the following two definitions

Definition 2 (Minimum Inter-Event Time for Agent i)**.** *For $j = \{SDTF, TDTF, MTF\}$, and for $i = \{1,\dots,n\}$ define the minimum inter-event time for Agent i Δ_j^i as* $\Delta_j^i \triangleq \min_k\{t_{k+1}^i - t_k^i\}$.

Definition 3 (Infimum Time of Δ_j^i For Agent i)**.** *For $j = \{SDTF, TDTF, MTF\}$, and for $i = \{1,\dots,n\}$, define the "infimum time of Δ_j^i for Agent i" as* $t_{\Delta_j^i} \triangleq \inf_{t_k^i} t_k^i : t_{k+2}^i - t_{k+1}^i = t_{k+1}^i - t_k^i = \Delta_j^i, \forall k$.

In other words, for Agent i, $t_{\Delta_j^i}$ is the infimum of all event times $t_k^i, \forall\, k$ such that the inter-event time between consecutive events $k+1$ and $k+2$ is equal to the minimum inter-event time Δ_j^i. If there are multiple consecutive events (e.g. 10 events) with inter-event time Δ_j^i then we call this a *dense triggering of events*. Note that $\Delta_j^i > 0$ for (22) and (23) because we can theoretically rule out Zeno behaviour. In these two cases, dense triggering is not Zeno behaviour, but is nevertheless undesirable.

Due to space limitations and the similarity of the proofs, we omit the proofs of convergence of system (7) under trigger functions (21) and (22). Figures 3 and 4 illustrate the controller (4) using SDTF (21), and TDTF (22), respectively. The figures show leader-follower consensus is achieved, the evolutions of comparison terms ($\beta_i\|\boldsymbol{v}_i(t)\|$ in SDTF and $\kappa_i\exp(-\varepsilon_i t)$ in TDTF) and event times. Figure 5 shows the performance of controller (4) using MTF. We also provide three tables to compare the trigger performance when using SDTF, TDTF and MTF. Table I records the total number of events which occur when using the three different trigger functions. Table II records the minimum inter-event time, Δ_j^i. Table III records the infimum time value, $t_{\Delta_j^i}$, which was defined in Definition 3 above.

Note that the SDTF and TDTF are widely adopted in event-based multi-agent consensus literature. We hereby review and illustrate the advantages and disadvantages regarding the trigger performance using SDTF and TDTF.

1) SDTF: The papers [14], [16], [22], [23], [35] used SDTF to determine the event times. The disadvantage of using SDTF is that Zeno behaviour can occur when the local state-dependent term crosses zero at a finite time value as indicated in [33] (i.e. in (21), the term $v_i(t) = 0$ instantaneously, for $t < \infty$). According to the first column of Table II, the minimum inter-event time is $\Delta_{\text{SDTF}}^i = 0.00005$ seconds, for all i, which is equal to the fixed time step of the MATLAB simulations. From the first column of Table III and the second sub-graph of Fig. 3, we observe that Zeno behaviour occurs at the time instants that $v_i(t)$ crosses 0, which supports the

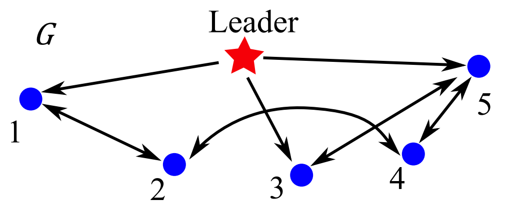

Fig. 1. Graph topology used in simulations

TABLE I
NUMBER OF EVENTS FOR THREE DIFFERENT TRIGGER FUNCTIONS

	State-dependent	Time-dependent	Mixed
Agent 1	259	5581	74
Agent 2	184	8106	63
Agent 3	575	2251	168
Agent 4	94	7365	101
Agent 5	438	3845	200
Total	1550	27148	606

TABLE II
MINIMUM INTER-EVENT TIME Δ_j^i UNDER THREE TRIGGER FUNCTIONS

	State-dependent	Time-dependent	Mixed
Agent 1	0.00005	0.00005	0.0388
Agent 2	0.00005	0.00005	0.0235
Agent 3	0.00005	0.00005	0.0010
Agent 4	0.00005	0.00005	0.0037
Agent 5	0.00005	0.00005	0.0006

TABLE III
THE INFIMUM TIME OF Δ_j, $t_{\Delta_j^i}$ AS DEFINED IN DEFINITION 3

	State-dependent	Time-dependent	Mixed
Agent 1	0.6736	29.8177	18.0246
Agent 2	0.3042	29.6469	2.3991
Agent 3	0.4722	29.8398	14.0583
Agent 4	1.3219	29.6458	1.3182
Agent 5	0.0798	29.9830	15.435

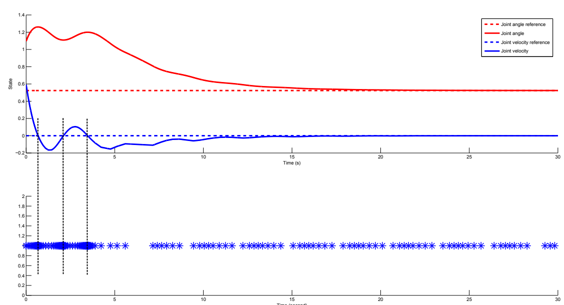

Fig. 2. Top: the evolutions of the generalized coordinate and velocity of agent 1. Bottom: the trigger event times of agent 1

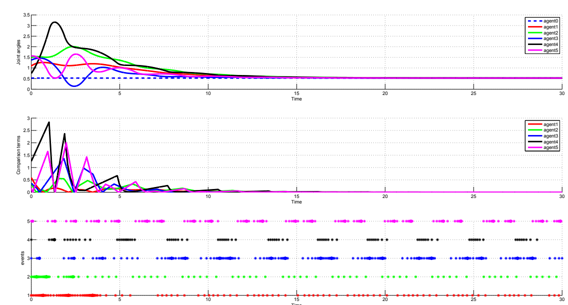

Fig. 3. Performance of controller (4) using SDTF (21). We set $\beta_i = 2.4$. From top to bottom: 1) the rendezvous of the generalized coordinates; 2) the evolution of $\beta_i\|v_i(t)\|$; 3) event times for each agent.

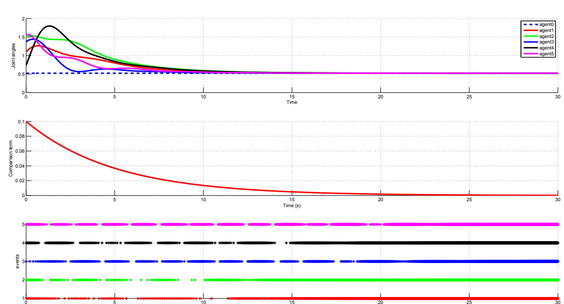

Fig. 4. Performance of controller (4) using TDTF (22). We set $\kappa_i \exp(-\varepsilon_i t) = 0.1\exp(-0.2t)$. From top to bottom: 1) the rendezvous of the generalized coordinates; 2) the evolution of $\kappa_i \exp(-\varepsilon_i t)$; 3) event times for each agent.

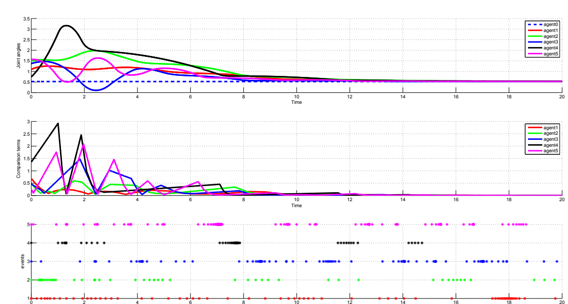

Fig. 5. Performance of controller (4) with MTF (23). We set $\beta_i = 2.4$ and $\kappa_i \exp(-\varepsilon_i t) = 0.1\exp(-0.2t)$. From top to bottom: 1) the rendezvous of the generalized coordinates; 2) the evolution of $\beta_i\|v_i(t)\| + \kappa_i \exp(-\varepsilon_i t)$; 3) event times for each agent.

conclusion of [33]. However, according to the arguments in [14], [33], if each agent uses SDTF, then at any time t, there exists at least one agent for which the next inter-event interval is strictly positive at any time t. In other words, for all $t \in [0, \infty)$, some agents may exhibit Zeno behaviour, *but at least one agent will have a constant lower bound on its inter-event time.*

2) TDTF: In [15], [36], [37], by using carefully-designed TDTF (typically the decay rate of ε_i in (22) must be upper bounded), a strictly positive and *constant lower bound* on the inter-event time interval for each agent can be obtained. However, the use of the TDTF has the following two limitations: 1) the applied system has to be exponentially stable, and 2) accurate model information (agent's dynamic model and network topology) is required to design the decay rate of $\exp(-\varepsilon_i t)$. We emphasise that the use of TDTF with arbitrary decay rate for $\exp(-\varepsilon_i t)$ is enough to exclude Zeno behaviour (see the second part of the proof of **Theorem** 2). However, if the decay rate is not selected to be sufficiently slow, the lower bound on the inter-event time cannot be guaranteed to be constant, but instead becomes time dependent. This results in dense triggering behaviour as consensus is almost reached, i.e. multiple events occur in a very short time interval (see Fig. 4). From the second columns of Table II and Table III, it is observed that Δ^i_{TDTF} occurs around $29s$, for all i, which is when the system is close to consensus. Note that dense triggering as $t \to \infty$ is not Zeno behaviour (See Definition 1). However, it can be observed from Table I that unsuitably chosen trigger function parameters will introduce a large amount of events, which is obviously undesirable. This is in contrast to the SDTF, which ensures that a constant lower bound exists on the inter-event time of at least one agent. In other words, a poorly designed TDTF will result in multiple events in sequence with inter-event time equal to Δ^i_{TDTF} when agents near consensus. In comparison SDTF ensures that for $t = [0, \infty)$, there will always be at least one agent whose inter-event time is lower bounded by a positive constant, even as agents near consensus. See Fig. 4 in comparison to Fig. 3.

3) MTF: According to Table I, it is straightforward to conclude that using MTF shows the best trigger performance with the least number of total events. According to Table I, using MTF also shows that the minimum inter-event time, Δ^i_{MTF} is greater than the constant MATLAB step size of 0.00005 seconds, which indicates Zeno behaviour is excluded. These observations reveal that MTF is able to combine the advantages of using SDTF and TDTF separately, i.e., the exclusion of Zeno behaviour in finite time (TDTF) and guarantee that dense triggering does not occur as consensus is reached (SDTF). This can also be observed from Fig. 5 in comparison to Fig. 3 and Fig. 4. We conducted a large number of simulations with arbitrarily chosen $\kappa_i \exp(-\varepsilon_i t)$, all of which show the above observations. However, a thorough analysis to find a *constant* lower bound on Δ^i_j when using MTF remains an open challenge (we can find a time-dependent bound).

Remark 5. *The intuition behind the MTF is straightforward. The time-dependent term $\kappa_i \exp(-\varepsilon_i t)$ (strictly positive for any $t < \infty$) in the MTF ensures that the error term $\|\boldsymbol{e}_i(t)\|$ will not compare to a zero threshold when the state-dependent term $\boldsymbol{v}_i(t)$ crosses zero, thus avoiding possible Zeno behaviour that may occur using SDTF. Meanwhile, by using numerical simulation examples, it is observed that using SDTF shows better trigger performance near consensus. Although theoretical explanations about this cannot be provided at this stage, simulations show that using MTF combines the benefits of separately using SDTF and TDTF.*

Note that it is not guaranteed that using MTF will always result in better trigger performance (larger Δ^j_i and fewer trigger events) compared to using SDTF or TDTF. For example, it is possible that $\boldsymbol{v}_i(t)$ does not cross zero at any $t < \infty$, depending on the initial conditions and network dynamics. In this case, Zeno behaviour will not occur even when using SDTF. Another example is that using a well-designed TDTF (suitably chosen decay rate ε_i based on accurate model knowledge) may also have better trigger performance than using MTF. Nevertheless, zero-crossing phenomenon cannot always be avoided when using SDTF and it is difficult to find a suitable TDTF in our proposed controller. In general, using MTF is the most suitable way for all three proposed event-triggered controllers.

Remark 6. *The work [38], [39] also use MTF. However, the authors design the evolution speeds of the exponential functions using exact knowledge of agent dynamic models and the graph topology. The effects of adding state-dependent terms to the trigger functions were not well-addressed by the authors of [38], [39].*

IV. Model-Independent Controller on Directed Graph

In this section, we propose and analyse a distributed event-triggered algorithm for a directed network where each fully-actuated agent has self-dynamics described by the Euler-Lagrange equation. For design of the control laws, the following assumption is required.

Assumption 2 (Limited Use of Centralised Design)**.** *Three parameters in the algorithm in this Section must be designed to exceed several lower bounding inequalities. These inequalities require knowledge of the constants $k_{\underline{m}}, k_{\overline{M}}, k_C$ defined in the properties P2 and P3 and the matrices $\boldsymbol{Q}$, $\mathcal{L}_{22}$ and $\boldsymbol{\Gamma}$ as defined in Lemma 3. We therefore assume these constants are known to the designer.*

Let the triggering time sequence of agent i be $t^i_0, t^i_1, \ldots, t^i_k, \ldots$ with $t^i_0 := 0$. Consider a model-independent, event-triggered algorithm for the i^{th} follower agent of the form

$$\boldsymbol{\tau}_i(t) = -\sum_{j \in \mathcal{N}_i} a_{ij}\Big((\boldsymbol{q}_i(t^i_k) - \boldsymbol{q}_j(t^i_k)) + \mu(\dot{\boldsymbol{q}}_i(t^i_k) - \dot{\boldsymbol{q}}_j(t^i_k))\Big)$$
$$t \in [t^i_k, t^i_{k+1}) \tag{24}$$

where a_{ij} is the weighted (i, j)th entry of the adjacency matrix $\mathcal{A}$ associated with the weighted directed graph $\mathcal{G}$. The control gain scalar $\mu > 0$ is universal to all agents. To ensure the control objective is achieved, μ must be designed to satisfy several inequalities, which will be detailed below. Note that if the leader is a neighbour of agent i then for $j = 0$ we have $\mu(\dot{\boldsymbol{q}}_i(t^i_k) - \dot{\boldsymbol{q}}_0(t^i_k)) = \mu(\dot{\boldsymbol{q}}_i(t^i_k))$, which is simply a damping term.

Define a new variable for agent i as

$$\boldsymbol{z}_i(t) = \sum_{j \in \mathcal{N}_i} a_{ij}\Big((\boldsymbol{q}_i(t) - \boldsymbol{q}_j(t)) + \mu(\dot{\boldsymbol{q}}_i(t) - \dot{\boldsymbol{q}}_j(t))\Big)$$

We define a state mismatch for agent i between consecutive event times t^i_k and t^i_{k+1} as follows:

$$\boldsymbol{e}_i(t) = \boldsymbol{z}_i(t^i_k) - \boldsymbol{z}_i(t)\,,\ t \in [t^i_k, t^i_{k+1}) \tag{25}$$

The trigger function is proposed as follows:

$$f_i(e_i(t)) = \|\boldsymbol{e}_i(t)\|^2 - \mu^{-2}{\beta_1}^2 \| \sum_{j\in\mathcal{N}_i} a_{ij}(\boldsymbol{q}_i(t) - \boldsymbol{q}_j(t))\|^2 \\ - {\beta_2}^2 \| \sum_{j\in\mathcal{N}_i} a_{ij}(\boldsymbol{v}_i(t) - \boldsymbol{v}_j(t))\|^2 - \omega_i(t) \tag{26}$$

where $\omega_i(t) = a_i \exp(-\kappa_i t)$ where $a_i, \kappa_i > 0$. The parameters β_1 and β_2 are to be determined in the sequel. The k^{th} event for agent i is triggered as soon as the trigger condition $f_i(\boldsymbol{e}_i(t)) = 0$ is fulfilled at $t = t_k^i$. For $t \in [t_k^i, t_{k+1}^i)$, the control input is $\tau_i(t) = \tau_i(t_k^i)$; the control input is updated when the next event is triggered. Furthermore, every time an event is triggered, and in accordance with their definitions, the measurement error $\boldsymbol{e}_i(t)$ is reset to be equal to zero and thus the trigger function assumes a non-positive value. One can immediately observe that for all t

$$\|\boldsymbol{e}_i(t)\|^2 \leq \mu^{-2}{\beta_1}^2 \| \sum_{j\in\mathcal{N}_i} a_{ij}(\boldsymbol{q}_i(t) - \boldsymbol{q}_j(t))\|^2 \\ + {\beta_2}^2 \| \sum_{j\in\mathcal{N}_i} a_{ij}(\boldsymbol{v}_i(t) + \boldsymbol{v}_j(t))\|^2 + \omega_i(t)$$

and note that $\sum_{j\in\mathcal{N}_i} a_{ij}(\boldsymbol{q}_i(t) - \boldsymbol{q}_j(t)) = \sum_{j\in\mathcal{N}_i} a_{ij}[(\boldsymbol{q}_i(t) - \boldsymbol{q}_0) - (\boldsymbol{q}_j(t) - \boldsymbol{q}_0)] = \boldsymbol{l}_i^\top \boldsymbol{u}$ where $\boldsymbol{l}_i^\top$ is the i^{th} row of $\mathcal{L}_{22}$. Likewise, $\sum_{j\in\mathcal{N}_i} a_{ij}(\boldsymbol{v}_i(t) - \boldsymbol{v}_j(t)) = \boldsymbol{l}_i^\top \boldsymbol{v}$. The stacked column vector $\boldsymbol{e} = [\boldsymbol{e}_1^\top, \ldots, \boldsymbol{e}_n^\top]^\top$ then has the following property

$$\|\boldsymbol{e}\|^2 = \sum_{i=1}^n \|\boldsymbol{e}_i(t)\|^2 \\ \leq \sum_{i=1}^n \Big(\mu^{-2}{\beta_1}^2 \|\boldsymbol{l}_i^\top \boldsymbol{u}\|^2 + {\beta_2}^2 \|\boldsymbol{l}_i^\top \boldsymbol{v}\|^2 + \omega_i(t) \Big) \tag{27}$$

It is straightforward to verify that $\sum_{i=1}^n \|\boldsymbol{l}_i^\top \boldsymbol{x}\|^2 = \|\mathcal{L}_{22}\boldsymbol{x}\|^2$, and $\sum_{i=1}^n \|\boldsymbol{l}_i^\top \boldsymbol{v}\|^2 = \|\mathcal{L}_{22}\boldsymbol{v}\|^2$. It then follows that

$$\|\boldsymbol{e}\|^2 \leq \mu^{-2}{\beta_1}^2 \|\mathcal{L}_{22}\boldsymbol{u}\|^2 + {\beta_2}^2 \|\mathcal{L}_{22}\boldsymbol{v}\|^2 + \bar{\omega}(t)^2 \tag{28}$$

$$\|\boldsymbol{e}\| \leq \mu^{-1}\beta_1 \|\mathcal{L}_{22}\|\|\boldsymbol{u}\| + \beta_2 \|\mathcal{L}_{22}\|\|\boldsymbol{v}\| + \bar{\omega}(t) \tag{29}$$

where $\bar{\omega}(t) = (\sum_{i=1}^n \omega_i(t))^{\frac{1}{2}}$.

It is obvious that

$$\boldsymbol{\tau}_i(t) = \boldsymbol{z}_i(t) + \boldsymbol{e}_i(t)$$

Applying control law (24) to each agent we can express the networked system using the variables $\boldsymbol{u}, \boldsymbol{v}$ defined below (8) as

$$\boldsymbol{M}(\boldsymbol{q})\dot{\boldsymbol{v}} + \boldsymbol{C}(\boldsymbol{q}, \boldsymbol{v})\boldsymbol{v} + (\mathcal{L}_{22} \otimes \boldsymbol{I}_p)(\boldsymbol{u} + \mu\boldsymbol{v}) + \boldsymbol{e} = \boldsymbol{0} \tag{30}$$

and expressed as the non-autonomous system

$$\dot{\boldsymbol{u}} = \boldsymbol{v} \\ \dot{\boldsymbol{v}} = -\boldsymbol{M}(\boldsymbol{q})^{-1} \left[\boldsymbol{C}(\boldsymbol{q}, \boldsymbol{v})\boldsymbol{v} + (\mathcal{L}_{22} \otimes \boldsymbol{I}_p)(\boldsymbol{u} + \mu\boldsymbol{v}) + \boldsymbol{e} \right] \tag{31}$$

By using arguments like those of usual Lyapunov theory, we will be able to prove the stability of (31). Before we present the main theorem of this section, we state a mild assumption used *only in this Section*.

Assumption 3. *All possible initial conditions lie in some fixed but arbitrarily large set, which is known a priori. In particular, $\|\boldsymbol{u}_i(0)\| \leq k_a/\sqrt{n}$ and $\|\boldsymbol{v}_i(0)\| \leq k_b/\sqrt{n}$, where k_a, k_b are known a priori.*

This assumption is entirely reasonable; many Euler-Lagrange systems will have an expected operating range for $\boldsymbol{q}$ and $\dot{\boldsymbol{q}}$.

Theorem 3. *Suppose that each follower agent with dynamics* (2)*, under Assumption 1, employs the controller* (24) *with trigger function* (26)*. Suppose further that the directed graph $\mathcal{G}$ contains a directed spanning tree, with the leader agent 0 as the root node (and thus with no incoming edges). Then there exists a sufficiently large μ, and sufficiently small β_1, β_2 which ensures that the leader-follower consensus objective is achieved semi-globally exponentially fast.*

Proof. The proof is lengthy and involves complex computations due to the combination of the highly nonlinear Euler-Lagrange dynamics, the directed graph, and the event-based controller. We shall provide a sketch of the proof here, and refer the reader to the appendix of [28] for the full proof.

Design of the control gains requires use of the quantities $k_a, k_b, k_C, k_{\underline{m}}, k_{\overline{M}}, \lambda_{\min}(\boldsymbol{Q})$, $\lambda_{\max}(\boldsymbol{Q})$, and $\boldsymbol{\Gamma}$, where $\boldsymbol{Q} = \boldsymbol{\Gamma}\mathcal{L}_{22} + \mathcal{L}_{22}^\top\boldsymbol{\Gamma} > 0$ as defined in Lemma 3. Let us define $\bar{\gamma}$ and $\underline{\gamma}$ as the largest and smallest entries of the diagonal, positive definite $\boldsymbol{\Gamma}$, and let δ be an arbitrarily small constant satisfying $k_{\underline{m}} - \delta > 0$.

Firstly, we compute two scalar quantities $\mathcal{X} > 0$ and $\mathcal{Y} > 0$ using $k_a, k_b, k_{\underline{m}}, k_{\overline{M}}, \lambda_{\min}(\boldsymbol{Q})$, $\lambda_{\max}(\boldsymbol{Q})$, and $\boldsymbol{\Gamma}$, and these two quantities have the property that $\|\boldsymbol{u}(0)\| < \mathcal{X}$ and $\|\boldsymbol{v}(0)\| < \mathcal{Y}$. In fact, a key part of the proof will be to show that $\|\boldsymbol{u}(t)\| < \mathcal{X}$ and $\|\boldsymbol{v}(t)\| < \mathcal{Y}$ holds for all $t \geq 0$. The control gain μ is involved in computing the quantities $\mathcal{X}$ and $\mathcal{Y}$, but it can be shown that if we use any $\mu \geq \mu_1$, where

$$\mu_1 = \max\left\{ \sqrt{\frac{\bar{\gamma}(k_{\overline{M}} + \delta)}{2\lambda_{\max}(\boldsymbol{Q})}}, \sqrt{\frac{2\underline{\gamma}(k_{\underline{m}} - \delta}{\lambda_{\min}(\boldsymbol{Q})}} \right\} \tag{32}$$

then $\mathcal{X}$ and $\mathcal{Y}$ are independent of μ. In other words, $\mathcal{X}$ and $\mathcal{Y}$ change with μ only if $\mu < \mu_1$.

We propose a Lyapunov-like function $V = \frac{1}{2}\boldsymbol{u}^\top\boldsymbol{Q}\boldsymbol{u} + \frac{1}{2}\boldsymbol{v}^\top\boldsymbol{\Gamma}_p\boldsymbol{M}\boldsymbol{v} + \mu^{-1}\boldsymbol{u}^\top\boldsymbol{\Gamma}_p\boldsymbol{M}\boldsymbol{v}$, where $\boldsymbol{\Gamma}_p = \boldsymbol{\Gamma} \otimes \boldsymbol{I}_p$. We show that V is positive definite and radially unbounded if $\mu > \mu_2 = \sqrt{\bar{\gamma}k_{\overline{M}}/\lambda_{\min}(\boldsymbol{Q})}$. We next analyse the derivative $\dot{V}$. First, let us define the following regions. For two scalars φ_0, ϑ_0 satisfying $\mathcal{X} - \vartheta_0 > 0$ and $\mathcal{Y} - \varphi_0 > 0$, define $\mathcal{U} = \{\|\boldsymbol{u}\|, \|\boldsymbol{v}\| : \|\boldsymbol{u}\| \in [\mathcal{X} - \vartheta_0, \mathcal{X}], \|\boldsymbol{v}\| \geq 0\}$ and $\mathcal{V} = \{\|\boldsymbol{u}\|, \|\boldsymbol{v}\| : \|\boldsymbol{u}\| \geq 0, \|\boldsymbol{v}\| \in\in [\mathcal{Y} - \varphi_0, \mathcal{Y}]\}$. Define further $\bar{\mathcal{U}} = \{\|\boldsymbol{u}\|, \|\boldsymbol{v}\| : \|\boldsymbol{u}\| > \mathcal{X}\}$ and $\bar{\mathcal{V}} = \{\|\boldsymbol{u}\|, \|\boldsymbol{v}\| : \|\boldsymbol{v}\| > \mathcal{Y}\}$. Lastly, we define $\mathcal{S} = (\mathcal{U} \cup \mathcal{V}) \cap (\bar{\mathcal{U}} \cup \bar{\mathcal{V}})$ and $\mathcal{T} = \{\|\boldsymbol{u}\|, \|\boldsymbol{v}\| : \|\boldsymbol{u}\| \in [0, \mathcal{X} - \vartheta_0), \|\boldsymbol{v}\| \in [0, \mathcal{Y} - \varphi_0)\}$, and this is the red and blue shaded region in Fig. 6, respectively.

In the extended proof in [28], we provide analytic expressions for a quantity μ_3 (which depends on $\mathcal{X}, \mathcal{Y}, k_C, \|\mathcal{L}_{22}\|, \lambda_{\min}(\boldsymbol{Q})$) and upper bounds on β_1 and β_2 (which are used in the trigger function (26)). We show that if $\mu \geq \mu_3$ and β_1, β_2 satisfy these upper bounds, then $\dot{V}$ is

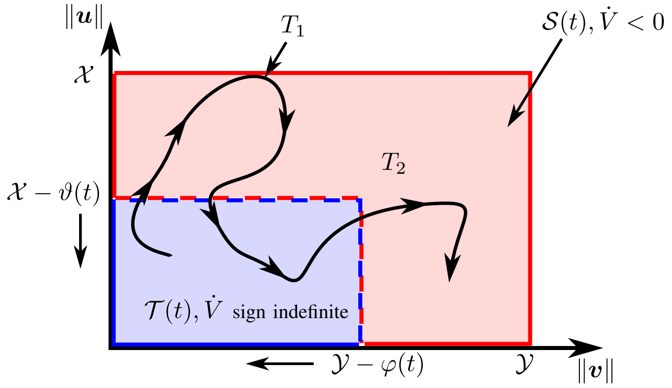

Fig. 6. Diagram for proof of **Theorem** 3. The red region is $\mathcal{S}(t)$, in which $\dot{V}(t) < 0$ for all $t \geq 0$. The blue region is $\mathcal{T}(t)$, in which $\dot{V}(t)$ is sign indefinite. A trajectory of (31) is shown with the black curve. At some time $t = T_1$, we show that the trajectory of (31) is such that $\|\boldsymbol{u}(T_1)\| < \mathcal{X}, \|\boldsymbol{v}(T_1)\| < \mathcal{Y}$ and thus the trajectory does not leave $\mathcal{S}(t)$. We show that $\vartheta(t)$ and $\varphi(t)$ monotonically increase until $\vartheta(t) = \mathcal{X}$ and $\varphi(t) = \mathcal{Y}$, at which point $\mathcal{T}(t) = \emptyset$. This corresponds to the dotted red and blue lines, which show, respectively, the time-varying boundaries of $\mathcal{S}(t)$ and $\mathcal{T}(t)$. The solid red and blue lines show respectively, the boundaries of $\mathcal{S}(t)$ and $\mathcal{T}(t)$, which are time-invariant. Lastly, we use the behaviour of $\mathcal{T}(t)$ and $\mathcal{S}(t)$ to conclude exponential convergence to the origin.

negative definite in $\mathcal{S}$ and sign indefinite in $\mathcal{T}$. Moreover, we show that $\|\boldsymbol{u}(t)\| < \mathcal{X}$ and $\|\boldsymbol{v}(t)\| < \mathcal{Y}$ holds for all time, i.e. the trajectories of the networked system are bounded. Lastly, we show that in fact, given a constant $\mu \geq \max\{\mu_1, \mu_2, \mu_3\}$, the region $\mathcal{S}(t)$ and $\mathcal{T}(t)$ are time-varying. This is because ϑ_0 and φ_0 in the above definition of $\mathcal{S}$ and $\mathcal{T}$ can be respectively replaced by strictly monotonically increasing functions $\vartheta(t)$ and $\varphi(t)$, while continuing to satisfy that $\dot{V} < 0$ in $\mathcal{S}(t)$ and $\dot{V}$ sign indefinite in $\mathcal{T}(t)$. The functions are are bounded as $\vartheta_0 \leq \vartheta(t) \leq \mathcal{X}$ and $\varphi_0 \leq \varphi(t) \leq \mathcal{Y}$. We then show that $\mathcal{T}(t)$ vanishes exponentially fast, so that $\mathcal{T}(\infty) = \emptyset$ and $\mathcal{S}(\infty) = \{\|\boldsymbol{u}\|, \|\boldsymbol{v}\| : \|\boldsymbol{u}\| \in [0, \mathcal{X}], \|\boldsymbol{v}\| \in [0, \mathcal{Y}]\}$. Lastly, we show that this implies the exponential convergence of the networked system (31) to $\boldsymbol{u} = \boldsymbol{v} = \boldsymbol{0}_{np}$, which indicates that leader-follower consensus is achieved. This completes the proof. □

V. Adaptive, model-dependent controller on directed network

In this section, we propose an adaptive, distributed event-triggered controller to achieve leader-follower consensus for a directed network of Euler-Lagrange agents. This allows for uncertain parameters in each agent, e.g. the mass of a robotic manipulator arm, and includes the gravitational forces.

Before we present the main results, we introduce variables which allow us to rewrite the multi-agent system in a way which facilitates stability analysis. A lemma on stability is also provided. To begin, we introduce the following auxiliary variables $\boldsymbol{q}_{ri}$ and $\boldsymbol{s}_i$, which appeared in [8], [40] studying leader-follower problems in directed Euler-Lagrange networks. Define

$$\dot{\boldsymbol{q}}_{ri}(t) = -\alpha \sum_{j=0}^{n} a_{ij}(\boldsymbol{q}_i(t) - \boldsymbol{q}_j(t)), \tag{33}$$

$$\boldsymbol{s}_i(t) = \dot{\boldsymbol{q}}_i(t) - \dot{\boldsymbol{q}}_{ri}(t) = \dot{\boldsymbol{q}}_i(t) + \alpha \sum_{j=0}^{n} a_{ij}(\boldsymbol{q}_i(t) - \boldsymbol{q}_j(t)), \quad i = 1, \ldots, n \tag{34}$$

where α is a positive constant, a_{ij} is the weighted (i, j) entry of the adjacency matrix $\mathcal{A}$ associated with the directed graph $\mathcal{G}$ that characterises the sensing flows among the n followers. Utilising **Lemma** 3, one can then verify that the compact form of (34) can be written as:

$$\dot{\boldsymbol{q}}(t) = -\alpha(\boldsymbol{\mathcal{L}}_{22} \otimes \boldsymbol{I}_p)(\boldsymbol{q}(t) - \boldsymbol{1}_n \otimes \boldsymbol{q}_0) + \boldsymbol{s}(t) \tag{35}$$

From P6 and the definition of $\dot{\boldsymbol{q}}_{ri}$, we obtain

$$\boldsymbol{M}_i(\boldsymbol{q}_i)\ddot{\boldsymbol{q}}_{ri} + \boldsymbol{C}_i(\boldsymbol{q}_i, \dot{\boldsymbol{q}}_i)\dot{\boldsymbol{q}}_{ri} + \boldsymbol{g}_i(\boldsymbol{q}_i) = \boldsymbol{Y}_i(\boldsymbol{q}_i, \dot{\boldsymbol{q}}_i, \ddot{\boldsymbol{q}}_{ri}, \dot{\boldsymbol{q}}_{ri})\boldsymbol{\Theta}_i, \quad i = 1, \ldots, n \tag{36}$$

Note that $\boldsymbol{\Theta}_i$ is an unknown but constant vector for agent i. Let $\hat{\boldsymbol{\Theta}}_i(t)$ be agent i's estimate of $\boldsymbol{\Theta}_i$ at time t. We update $\hat{\boldsymbol{\Theta}}_i(t)$ by the following adaptation law:

$$\dot{\hat{\boldsymbol{\Theta}}}_i(t) = -\boldsymbol{\Lambda}_i \boldsymbol{Y}_i^\top(t)\boldsymbol{s}_i(t), \quad i = 1, \ldots, n \tag{37}$$

where $\boldsymbol{\Lambda}_i$ is a symmetric positive-definite matrix.

The control algorithm is now proposed. Let the triggering time sequence of agent i be $t_0^i, t_1^i, \ldots, t_k^i, \ldots$ with $t_0^i := 0$. The event-triggered controller for follower agent i is designed as:

$$\boldsymbol{\tau}_i(t) = -\boldsymbol{K}_i \boldsymbol{s}_i(t_k^i) + \boldsymbol{Y}_i(t_k^i)\hat{\boldsymbol{\Theta}}_i(t_k^i), \tag{38}$$

$$i = 1, \ldots, n, \quad t \in [t_k^i, t_{k+1}^i) \tag{39}$$

where $\boldsymbol{K}_i > 0$ is a symmetric positive definite gain matrix. It is observed that the control torque remains constant in the time interval $[t_k^i, t_{k+1}^i)$, i.e. $\boldsymbol{\tau}_i(t)$ is a piecewise-constant function in time. From the definitions of $\boldsymbol{q}_{ri}$ and $\boldsymbol{s}_i$, calculations show that the system in (1) can be written as

$$\boldsymbol{M}_i(\boldsymbol{q}_i)\dot{\boldsymbol{s}}_i(t) + \boldsymbol{C}_i(\boldsymbol{q}_i, \dot{\boldsymbol{q}}_i)\boldsymbol{s}_i(t) = -\boldsymbol{K}_i \boldsymbol{s}_i(t_k^i) + \boldsymbol{Y}_i(t_k^i)\hat{\boldsymbol{\Theta}}_i(t_k^i) - \boldsymbol{Y}_i(t)\boldsymbol{\Theta}_i \tag{40}$$

Before the trigger function is presented, we define two types of measurement error:

$$\begin{aligned} \boldsymbol{e}_i(t) &= \boldsymbol{s}_i(t_k^i) - \boldsymbol{s}_i(t); \\ \boldsymbol{\varepsilon}_i(t) &= \boldsymbol{Y}_i(t_k^i)\hat{\boldsymbol{\Theta}}_i(t_k^i) - \boldsymbol{Y}_i(t)\hat{\boldsymbol{\Theta}}_i(t); \end{aligned} \tag{41}$$

The trigger function is proposed as follows:

$$f_i(\boldsymbol{\varepsilon}_i(t), \boldsymbol{e}_i(t), \omega_i(t)) = \|\boldsymbol{\varepsilon}_i(t)\| + \lambda_{\max}(\boldsymbol{K}_i)\|\boldsymbol{e}_i(t)\| - \frac{\gamma_i}{2}\lambda_{\min}(\boldsymbol{K}_i)\|\boldsymbol{s}_i(t)\| - \omega_i(t) \tag{42}$$

where $0 < \gamma_i < 1$, $\omega_i(t) = \sigma_i\sqrt{\lambda_{\min}(\boldsymbol{K}_i)}\exp(-\kappa_i t)$ with $\sigma_i, \kappa_i > 0$. The k^{th} event for agent i is triggered as soon as the trigger condition $f_i(\boldsymbol{\varepsilon}_i(t), \boldsymbol{e}_i(t)) = 0$ is fulfilled at $t = t_k^i$. For $t \in [t_k^i, t_{k+1}^i)$, the control input is $\boldsymbol{\tau}_i(t) = \boldsymbol{\tau}_i(t_k^i)$; the control input is updated when the next event is triggered. Furthermore, every time an event is triggered, and in accordance with their definitions, the measurement errors $\varepsilon_i(t)$ and $e_i(t)$ are reset to be equal to zero. Thus $f_i(\epsilon_i(t), e_i(t), \omega_i(t)) \leq 0$ for all $t \geq 0$.

We now present our main result.

Theorem 4. *Consider the multi-agent system* (1) *with control law* (39)*. If $\mathcal{G}$ contains a directed spanning tree with the leader as the root vertex (and thus with no incoming edges), then leader-follower consensus is globally asymptotically achieved as $t \to \infty$ and no agent will exhibit Zeno behaviour.*

Proof. The proof is omitted due to space limitations, and can be found in [28]. □

VI. Conclusions

This paper proposed and showed the stability of three different algorithms for achieving leader-follower consensus for a network of Euler-Lagrange agents. Each algorithm is suited for a different scenario and have their advantages and disadvantages, and can be chosen depending on the problem requirements. For each algorithm, we propose a mixed trigger function. The effectiveness of such a mixed trigger function is extensively explained via simulations. Future work includes relaxation of the continuous sensing requirement to allow for event-based sensing. One possible approach is via self-triggered controllers, but this may be difficult due to the complex Euler-Lagrange dynamics. A second key future work is to obtain a constant lower bound on the inter-event times (currently the lower bound decreases as time increases).

Acknowledgements

The authors would like to acknowledge Prof. Brian D.O. Anderson for his invaluable discussions on stability of non-autonomous systems, and thank the Editor and anonymous reviewers for their comments and suggestions which improved the paper.

The work of Q. Liu, M. Ye and C. Yu was supported by the Australian Research Council (ARC) under the ARC grants DP-130103610 and DP-160104500, by the National Natural Science Foundation of China (grant 61375072) and a China Scholarship Council PhD scholarship.

The work of J. Qin was supported in part by the National Natural Science Foundation of China under Grant 61473269 and in part by the Youth Innovation Promotion Association of Chinese Academy of Sciences.

References

[1] Y. Cao, W. Yu, W. Ren, and G. Chen, "An Overview of Recent Progress in the Study of Distributed Multi-Agent Coordination," *IEEE Transactions on Industrial Informatics*, vol. 9, pp. 427–438, Feb 2013.

[2] L. Ding, Q.-L. Han, and G. Guo, "Network-based leader-following consensus for distributed multi-agent systems," *Automatica*, vol. 49, no. 7, pp. 2281–2286, 2013.

[3] L. Ding and W. X. Zheng, "Consensus tracking in heterogeneous nonlinear multi-agent networks with asynchronous sampled-data communication," *Systems & Control Letters*, vol. 96, pp. 151–157, 2016.

[4] R. Kelly, V. S. Davila, and J. A. L. Perez, *Control of robot manipulators in joint space*. Springer Science & Business Media, 2006.

[5] R. Ortega, J. A. L. Perez, P. J. Nicklasson, and H. Sira-Ramirez, *Passivity-based Control of Euler-Lagrange systems: Mechanical, Electrical and Electromechanical Applications*. Springer Science & Business Media, 2013.

[6] W. Ren and Y. Cao, *Distributed Coordination of Multi-agent Networks: Emergent Problems, Models and Issues*. Springer London, 2011.

[7] M. Ye, C. Yu, and B. D. O. Anderson, "Model-Independent Rendezvous of Euler-Lagrange Agents on Directed Networks," in *Proceedings of IEEE 54th Annual Conference on Decision and Control, Osaka, Japan*, pp. 3499–3505, 2015.

[8] J. Mei, W. Ren, J. Chen, and G. Ma, "Distributed adaptive coordination for multiple lagrangian systems under a directed graph without using neighbors velocity information," *Automatica*, vol. 49, no. 6, pp. 1723–1731, 2013.

[9] G. Guo, L. Ding, and Q.-L. Han, "A distributed event-triggered transmission strategy for sampled-data consensus of multi-agent systems," *Automatica*, vol. 50, no. 5, pp. 1489–1496, 2014.

[10] J. Qin, Q. Ma, Y. Shi, and L. Wang, "Recent advances in consensus of multi-agent systems: A brief survey," *IEEE Transactions on Industrial Electronics*, 2016.

[11] H. Li, S. Liu, Y. C. Soh, and L. Xie, "Event-triggered communication and data rate constraint for distributed optimization of multiagent systems," *IEEE Transactions on Systems, Man, and Cybernetics: Systems*, 2017.

[12] J. Zhang, K. H. Johansson, J. Lygeros, and S. Sastry, "Zeno hybrid systems," *International Journal of Robust and Nonlinear Control*, vol. 11, no. 5, pp. 435–451, 2001.

[13] A. D. Ames, P. Tabuada, and S. Sastry, "On the stability of zeno equilibria," in *International Workshop on Hybrid Systems: Computation and Control*, pp. 34–48, Springer, 2006.

[14] D. V. Dimarogonas, E. Frazzoli, and K. H. Johansson, "Distributed event-triggered control for multi-agent systems," *Automatic Control, IEEE Transactions on*, vol. 57, no. 5, pp. 1291–1297, 2012.

[15] G. S. Seyboth, D. V. Dimarogonas, and K. H. Johansson, "Event-based broadcasting for multi-agent average consensus," *Automatica*, vol. 49, no. 1, pp. 245–252, 2013.

[16] Y. Fan, G. Feng, Y. Wang, and C. Song, "Distributed event-triggered control of multi-agent systems with combinational measurements," *Automatica*, vol. 49, no. 2, pp. 671–675, 2013.

[17] Q. Liu, J. Qin, and C. Yu, "Event-based multi-agent cooperative control with quantized relative state measurements," in *Decision and Control, 2016. 55th IEEE Conference on*, pp. 2233 – 2239, IEEE, 2016.

[18] B. Mu, H. Li, W. Li, and Y. Shi, "Consensus for multiple euler-lagrange dynamics with arbitrary sampling periods and event-triggered strategy," in *Intelligent Control and Automation (WCICA), 2014 11th World Congress on*, pp. 2596–2601, IEEE, 2014.

[19] N. Huang, Z. Duan, and Y. Zhao, "Distributed consensus for multiple Euler-Lagrange systems: An event-triggered approach," *Science China: Technological Sciences*, vol. 59, pp. 33–44, January 2016.

[20] Z. Meng and Z. Lin, "Distributed Finite-time Cooperative Tracking of Networked Lagrange Systems via Local Interactions," in *American Control Conference (ACC), Montréal, Canada*, pp. 4951–4956, IEEE, 2012.

[21] J. Mei, W. Ren, and G. Ma, "Distributed Coordinated Tracking With a Dynamic Leader for Multiple Euler-Lagrange Systems," *IEEE Transactions on Automatic Control*, vol. 56, no. 6, pp. 1415–1421, 2011.

[22] X. Liu, C. Du, P. Lu, and D. Yang, "Decentralised consensus for multiple lagrangian systems based on event-triggered strategy," *International Journal of Control*, vol. 89, no. 6, pp. 1111–1124, 2016.

[23] E. Garcia, Y. Cao, H. Yu, P. Antsaklis, and D. Casbeer, "Decentralised event-triggered cooperative control with limited communication," *International Journal of Control*, vol. 86, no. 9, pp. 1479–1488, 2013.

[24] J. Mei, W. Ren, J. Chen, and B. D. O. Anderson, "Consensus of linear multi-agent systems with fully distributed control gains under a general directed graph," in *IEEE 53rd Annual Conference on Decision and Control*, (Los Angeles, USA), pp. 2993–2998, IEEE, 2014.

[25] J. Mei, W. Ren, and J. Chen, "Distributed Consensus of Second–Order Multi–Agent Systems with Heterogeneous Unknown Inertias and Control Gains Under a Directed Graph," *IEEE Transactions on Automatic Control*, vol. 61, no. 8, pp. 2019–2034, 2016.

[26] Z. Li and Z. Duan, *Cooperative Control of Multi-Agent Systems: A Consensus Region Approach*. CRC Press, 2014.

[27] Q. Liu, M. Ye, J. Qin, and C. Yu, "Event-based leader-follower consensus for multiple Euler-Lagrange systems with parametric uncertainties," in *Proceedings of IEEE 55th Annual Conference on Decision and Control (CDC), Las Vegas, USA*, pp. 2240–2246.

[28] Q. Liu, M. Ye, J. Qin, and C. Yu, "Event-triggered algorithms for leader-follower consensus of networked euler-lagrange agents." https://arxiv.org/abs/1705.07305, 2017. [Online].

[29] W. Rudin *et al.*, *Principles of mathematical analysis*, vol. 3. McGraw-Hill New York, 1964.

[30] P. A. Ioannou and B. Fidan, *Adaptive Control Tutorial*. SIAM, 2006.

[31] Q. Song, F. Liu, J. Cao, and W. Yu, "Pinning-controllability analysis of complex networks: an m-matrix approach," *Circuits and Systems I: Regular Papers, IEEE Transactions on*, vol. 59, no. 11, pp. 2692–2701, 2012.

[32] Z. Li, W. Ren, X. Liu, and M. Fu, "Consensus of Multi-Agent Systems With General Linear and Lipschitz Nonlinear Dynamics Using Distributed Adaptive Protocols," *IEEE Transactions on Automatic Control*, vol. 58, no. 7, pp. 1786–1791, 2013.

[33] Z. Sun, N. Huang, B. D. Anderson, and Z. Duan, "A new distributed zeno-free event-triggered algorithm for multi-agent consensus," in *Decision and Control (CDC), 2016 IEEE 55th Conference on*, pp. 3444–3449, IEEE, 2016.

[34] H. Li, X. Liao, T. Huang, and W. Zhu, "Event-triggering sampling based leader-following consensus in second-order multi-agent systems," *Automatic Control, IEEE Transactions on*, vol. 60, pp. 1998–2003, July 2015.

[35] W. Hu, L. Liu, and G. Feng, "Consensus of linear multi-agent systems by distributed event-triggered strategy," *IEEE Transactions on Cybernetics*, vol. 46, pp. 148–157, Jan 2016.

[36] D. Yang, W. Ren, X. Liu, and W. Chen, "Decentralized event-triggered consensus for linear multi-agent systems under general directed graphs," *Automatica*, vol. 69, pp. 242–249, 2016.

[37] B. Wei, F. Xiao, and M.-Z. Dai, "Edge event-triggered control for multi-agent systems under directed communication topologies," *International Journal of Control*, pp. 1–10, 2017.

[38] W. Zhu and Z.-P. Jiang, "Event-based leader-following consensus of multi-agent systems with input time delay," *IEEE Transactions on Automatic Control*, vol. 60, no. 5, pp. 1362–1367, 2015.

[39] X.-F. Wang, Z. Deng, S. Ma, and X. Du, "Event-triggered design for multi-agent optimal consensus of euler-lagrangian systems," *Kybernetika*, vol. 53, no. 1, pp. 179–194, 2017.

[40] J. Mei, W. Ren, and G. Ma, "Distributed Containment Control for Lagrangian Networks With Parametric Uncertainties Under a Directed Graph," *Automatica*, vol. 48, no. 4, pp. 653–659, 2012.

Qingchen Liu received both B.E. and M.E. degrees in control engineering from Harbin Engineering University, Harbin, China. He is currently pursuing the Ph.D. degree in control engineering at the Australian National University, Canberra, Australia.

His current research interests include distributed event-triggered control and coverage control for mobile sensing networks.

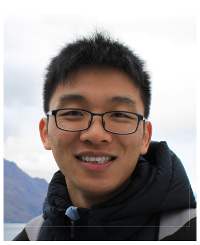

Mengbin Ye was born in Guangzhou, China. He received the B.E. degree (with First Class Honours) in mechanical engineering from the University of Auckland, Auckland, New Zealand. He is currently pursuing the Ph.D. degree in control engineering at the Australian National University, Canberra, Australia.

His current research interests include opinion dynamics and social networks, consensus and synchronisation of Euler-Lagrange systems, and localisation using bearing measurements.

Jiahu Qin (M'12) received the first Ph.D. degree in control science and engineering from the Harbin Institute of Technology, China, in 2012, and the second Ph.D. degree in systems and control from the Australian National University, Australia, in 2014. He is currently a Professor with the Department of Automation, University of Science and Technology of China, Hefei, China. His current research interests include consensus and coordination in multi-agent systems as well as complex network theory and its application.

Changbin Yu was born in Shandong, China. He received the B.Eng. degree with first class honors in computer engineering from Nanyang Technological University (NTU), Singapore in 2004, and a Ph.D. from the Australian National University (ANU) in 2008; since then he has been a faculty member of the ANU Research School of Engineering. In 2017 he become the first engineering faculty member joining the Westlake Institute for Advanced Study, and helping to establish the first private research-oriented university in China - Westlake University, Hangzhou, Zhejiang. He was a recipient of an 2010 ANU Top Supervisor Award, an 20062008 Asian Journal of Control Best Paper Award, an ARC Australian Postdoctoral Fellowship in 2007 and a Queen Elizabeth II Fellowship in 2010, a 2006 Chinese Government Award for Outstanding Students Abroad, an 2005 Australian Governments Endeavor Asia Award. He is a Fellow of Institution of Engineers Australia, a Senior Member of IEEE and a member of IFAC Technical Committee on Networked Systems.